Inorganic Chemistry

Article

pubs.acs.org/IC

Stepwise Expansion of Pd Chains from Binuclear Palladium(I) Complexes Supported by Tetraphosphine Ligands

Tomoaki Tanase,* Satoko Hatada, Sayo Noda, Hiroe Takenaka, Kanako Nakamae, Bunsho Kure, and Takayuki Nakajima

Department of Chemistry, Faculty of Science, Nara Women's University, Kitauoya-nishi-machi, Nara, 630-8506, Japan

Supporting Information

ABSTRACT: Reaction of $[Pd_2(XylNC)_6]X_2$ (X = PF_6, BF_4) with a linear tetraphosphine, *meso*-bis[(diphenylphosphinomethyl)-phenylphosphino]methane (dpmppm), afforded binuclear Pd^I complexes, $[Pd_2(\mu\text{-dpmppm})_2]X_2$ ($[\mathbf{2}]X_2$), through an asymmetric dipalladium complex, $[Pd_2(\mu\text{-dpmppm})(XylNC)_3]^{2+}$ ($[\mathbf{1}]^{2+}$). Complex $[\mathbf{2}]^{2+}$ readily reacted with $[Pd^0(dba)_2]$ (2 equiv) and an excess of isocyanide, RNC (R = 2,6-xylyl (Xyl), *tert*-butyl (^{t}Bu)), to generate an equilibrium mixture of $[Pd_4(\mu\text{-dpmppm})_2(RNC)_2]^{2+}$ ($[\mathbf{3}']^{2+}$) + RNC ⇄ $[Pd_4(\mu\text{-dpmppm})_2(RNC)_3]^{2+}$ ($[\mathbf{3}]^{2+}$), from which $[Pd_4(\mu\text{-dpmppm})_2(XylNC)_3]^{2+}$ ($[\mathbf{3a}]^{2+}$) and $[Pd_4(\mu\text{-dpmppm})_2(^t BuNC)_2]^{2+}$ ($[\mathbf{3b}']^{2+}$) were isolated. Variable-temperature UV−vis and $^{31}P\{^1H\}$ and ^1H NMR spectroscopic studies on the equilibrium mixtures demonstrated that the tetrapalladium complexes are quite fluxional in the solution state: the symmetric Pd_4 complex $[\mathbf{3b}']^{2+}$ predominantly existed at higher temperatures (>0 °C), and the equilibrium shifted to the asymmetric Pd_4 complex $[\mathbf{3b}]^{2+}$ at a low temperature (∼−30 °C). The binding constants were determined by UV−vis titration at 20 °C and revealed that XylNC is of higher affinity to the Pd_4 core than ^{t}BuNC. In addition, both isocyanides exhibited higher affinity to the electron deficient $[Pd_4(\mu\text{-dpmppmF}_2)_2(RNC)_2]^{2+}$ ($[\mathbf{3F}']^{2+}$) than to $[Pd_4(\mu\text{-dpmppm})_2(RNC)_2]^{2+}$ ($[\mathbf{3}']^{2+}$) (dpmppmF$_2$ = *meso*-bis[{di(3,5-difluorophenyl)phosphinomethyl}phenylphosphino]methane). When $[\mathbf{2}]X_2$ was treated with $[Pd^0(dba)_2]$ (2 equiv) in the absence of RNC in acetonitrile, linearly ordered octapalladium chains, $[Pd_8(\mu\text{-dpmppm})_4(CH_3CN)_2]X_4$ ($[\mathbf{4}]X_4$: X = PF_6, BF_4), were generated through a coupling of two $\{Pd_4(\mu\text{-dpmppm})_2\}^{2+}$ fragments. Complex $[\mathbf{2}]^{2+}$ was also proven to be a good precursor for Pd_2M_2 mixed-metal complexes, yielding $[Pd_2Cl(Cp^*MCl)(Cp^*MCl_2)(\mu\text{-dpmppm})_2]^{2+}$ (M = Rh ($[\mathbf{5}]^{2+}$), Ir ($[\mathbf{6}]^{2+}$), and $[Au_2Pd_2Cl_2(dpmppm{-}H)_2]^{2+}$ ($[\mathbf{7}]^{2+}$) by treatment with $[Cp^*MCl_2]_2$ and $[AuCl(PPh_3)]$, respectively. Complex $[\mathbf{7}]^{2+}$ contains an unprecedented PC(sp^3)P pincer ligand with a PCPCPCP backbone, dpmppm−H of deprotonated dpmppm. The present results demonstrated that the binuclear Pd^I complex $[\mathbf{2}]^{2+}$ was a quite useful starting material to extend the palladium chains and to construct Pd-involved heteromultinuclear systems.

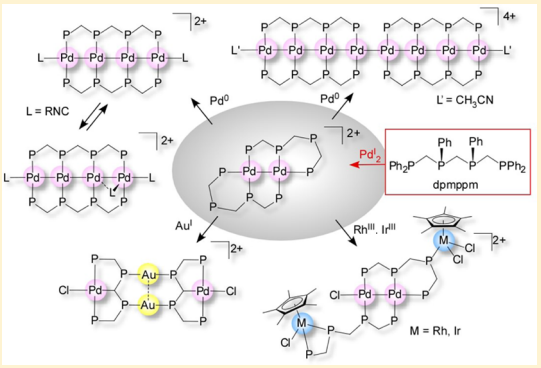

INTRODUCTION

Low-valent extended metal atom chains have been regarded as a promising molecular motif for down-sizing electronic devices made of metallic materials.[1] However, examples of the molecular metal chains including zerovalent metal atoms were limited to linear Pt_4 and Pd_4 complexes supported by bis-isocyanide[2] and linear palladium complexes (Pd_4, Pd_5) sandwiched by π-conjugated polyenes and perylenes.[3,4] Recently, further elongated chains of Ni_{11}[5] and Pd_{10}[6] have been developed by utilizing linearly designed template ligands, tetranaphthyridyltriamide and β-carotene, respectively, which are recognized as the longest molecular metal atom chains.

In contrast to the template synthesis, we have developed a methodology by which linear multinuclear metal building blocks are connected to extend low-valent Pt and Pd strings. A linear triphosphine, bis(diphenylphosphinomethyl)-phenylphosphine (dpmp),[7,8] has been proven very effective for stabilizing linear Pt_2M centers of $[Pt_2M(\mu\text{-dpmp})_2(RNC)_2](PF_6)_2$ (M = Pt, Pd),[7a] which readily undergo reductive coupling to generate a series of hydride-bridged linear $Pt_2M(\mu\text{-H})MPt_2$ hexanuclear clusters, $[Pt_4M_2(\mu\text{-H})(\mu\text{-dpmp})_4(RNC)_2]^{3+}$ (M = Pt, Pd; R = 2,6-xylyl (Xyl), 2,4,6-mesityl (Mes), *tert*-butyl (^{t}Bu)), $[Pt_6(\mu\text{-H})(\mu\text{-dpmp})_4(CO)_2]^{3+}$, and $[Pt_6(\mu\text{-H})X_2(\mu\text{-dpmp})_4]^+$ (X = H, I).[8] The hexanuclear strings are redox-active, and their two-electron oxidation afforded $[Pt_4M_2(\mu\text{-dpmp})_4(XylNC)_2](PF_6)_4$ (M = Pt, Pd), during which the $Pt_2M_2Pt_2$ hexanuclear strings were retained against the apparent hydride dissociation from the central part.[8c]

Recently, we synthesized a methylene-bridged linear tetraphosphine, *meso*-bis[(diphenylphosphinomethyl)-phenylphosphino]methane (dpmppm),[9,10] and have been successful in establishing low-valent octapalladium chains supported by dpmppm (Scheme 1a).[11] Reaction of the tetraphosphine with 2 equiv of $[Pd(dba)_2]$ in the presence of

Received: April 28, 2015
Published: August 12, 2015

DOI: 10.1021/acs.inorgchem.5b00950
Inorg. Chem. 2015, 54, 8298−8309

Scheme 1. (a) Preparations of Octapalladium Complexes Supported by Dpmppm Ligands and (b) Tetranuclear Palladium Complexes with $dpmppmF_2$ Ligands Showing Interconversion between the Symmetrical and Asymmetrical Structures

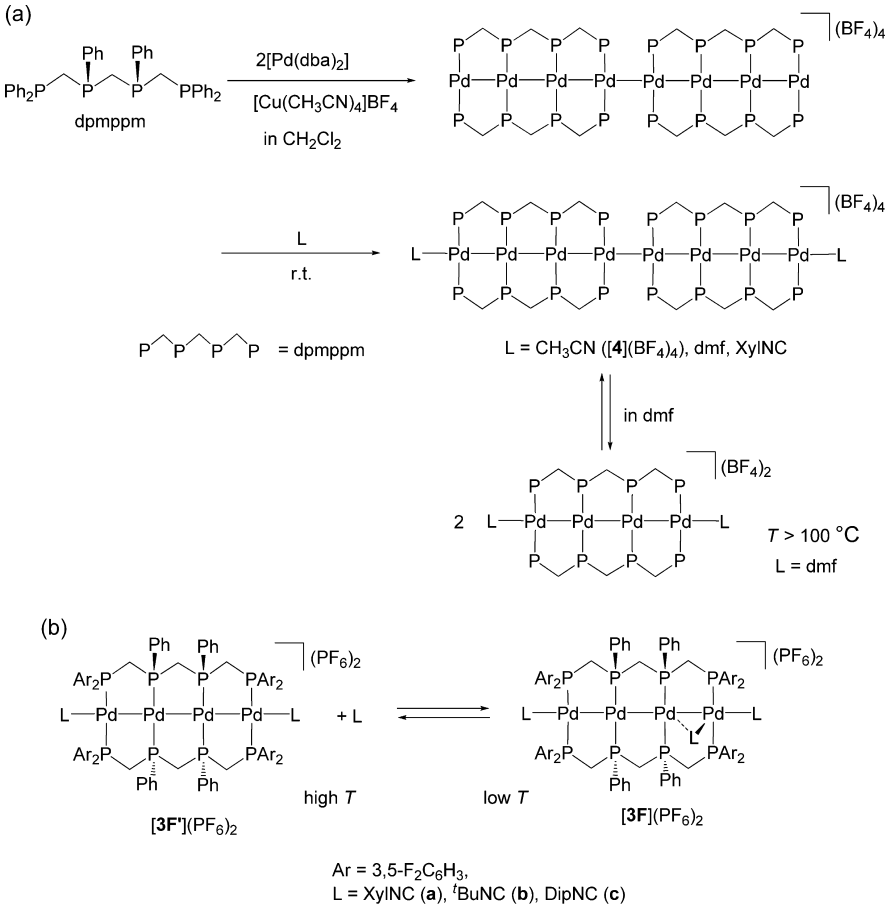

Cu^{I} species yielded a coordinatively unsaturated Pd_8 rod, $[Pd_8(\mu\text{-dpmppm})_4](BF_4)_4$, to the vacant terminal sites of which neutral two-electron donor ligands such as isocyanides and coordinative solvent molecules were readily incorporated to form the terminal-capped $[Pd_8(\mu\text{-dpmppm})_4(L)_2](BF_4)_4$ (L = XylNC, CH_3CN ([**4**](BF$_4$)$_4$), *N*,*N*-dimethylformamide (dmf)). These Pd_8 chains exhibited interesting temperature-dependent thermochromics behaviors with near IR absorptions (~900 nm) arising from a spin-allowed HOMO−LUMO transition. While variable temperature (VT) $^{31}P\{^1H\}$ NMR spectra indicated that the octapalladium chains were stable even in acetonitrile solutions below 60 °C, the Pd_8 chain dissociated into two Pd_4 fragments at higher temperatures above 100 °C in dmf, and when the temperature decreased below 60 °C, they were self-aligned to restore the Pd_8 string. These observations may imply a possibility of further aggregation of the Pd_4 units that could lead to unit-incremental expansion of palladium chains. These studies demonstrated potential importance of the Pd_4 units supported by dpmppm ligands, but it has not been successful to isolate the postulated complexes with a $\{Pd_4(\mu\text{-dpmppm})_2\}^{2+}$ core owing to their high instability. A linear tetraphosphine containing electron-withdrawing substituent groups, *meso*-bis{[di(3,5-difluorophenyl)phosphinomethyl]-phenylphosphino}methane ($dpmppmF_2$),[12] was prepared to tune electronic structures of the low-valent Pd_4 chain, and actually, $dpmppmF_2$ was very effective to stabilize the $\{Pd_4\}^{2+}$ chain, leading to successful isolation of $[Pd_4(\mu\text{-dpmppmF}_2)_2(RNC)_3](PF_6)_2$ ([**3F**](PF$_6$)$_2$; R = Xyl, Mes, 2,6-diisopropylphenyl (Dip), and ^{t}Bu; Scheme 1b). The isolated Pd_4 complexes showed interesting dynamic behaviors in the solutions states, which were related to dissociation into the symmetric $[Pd_4(\mu\text{-dpmppmF}_2)_2(RNC)_2](PF_6)_2$ ([**3F′**](PF$_6$)$_2$) and RNC through a structure−valence coupled interconversion between $Pd^0{\rightarrow}Pd^I{-}Pd^0{-}Pd^I$ (60 cluster valence electrons (CVEs)) and $Pd^I{-}Pd^0{-}Pd^0{-}Pd^I$ arrays (58 CVEs).[12] The tetraphosphine dpmppm has also proven very suitable for assembly of linear tetranuclear metal chains of group 11 metal ions (Au^I, Ag^I, Cu^I)[9a−d] and heterometallic octanuclear rings of $\{[Au_2MCuCl_2(\mu\text{-dpmppm})_2]_2\}^{4+}$ (M = Au, Ag, Cu).[9e] Furthermore, it can organize stepwise assembling of the heterotrinuclear metal ions of $[PdCl_2(Cp^*M'Cl_2)(Cp^*MCl_2)(\mu\text{-dpmppm-}\kappa^2,\kappa^1,\kappa^1)]$ and $[PdCl(\mu\text{-Cl})(Cp^*M'Cl)(Cp^*MCl_2)(\mu\text{-dpmppm-}\kappa^2,\kappa^1,\kappa^1)]^+$ (M, M′ = Rh, Ir; Cp* = pentamethylcyclopentadienyl).[9f] These studies demonstrated potential versatility of multimetallic structures constructed by the dpmppm ligands.

In the present study, we have synthesized binuclear Pd^I complexes supported by two dpmppm ligands, $[Pd_2(\mu\text{-dpmppm})_2]X_2$ ([**2**]X$_2$: X = PF_6, BF_4), and examined their reactions with various metal species to disclose that the binuclear Pd^I complex $[\mathbf{2}]^{2+}$ was a quite useful starting material to extend the palladium chains to Pd_4 and Pd_8 as $[Pd_4(\mu\text{-dpmppm})_2(RNC)_n]^{2+}$ (n = 2, 3) and $[Pd_8(\mu\text{-dpmppm})_4(CH_3CN)_2]^{4+}$ and to construct Pd-involved hetero-multinuclear systems of Pd_2M_2 (M = Rh, Ir) and Au_2Pd_2 complexes, $[Pd_2Cl(Cp^*MCl)(Cp^*MCl_2)(\mu\text{-dpmppm})_2]^{2+}$ (M

DOI: 10.1021/acs.inorgchem.5b00950
Inorg. Chem. 2015, 54, 8298−8309

= Rh, Ir) and $[Au_2Pd_2Cl_2(dpmppm-H)_2]^{2+}$, in stepwise procedures.

RESULTS AND DISCUSSION

Preparation of Binuclear Palladium(I) Complexes Supported by Tetraphosphine Ligands, $[Pd_2(\mu\text{-dpmppm})_2]X_2$ (X = PF_6, BF_4). When 2 equiv of dpmppm was reacted with dipalladium(I) isocyanide complex $[Pd_2(XylNC)_6]X_2$ (X = PF_6, BF_4) in dichloromethane, orange Pd^I_2 complexes formulated as $[Pd_2(\mu\text{-dpmppm})_2]X_2$ ($[\mathbf{2}]X_2$: X = PF_6, BF_4) were isolated in good yields (Scheme 2). The ESI

Scheme 2. Reactions of dpmppm with $[Pd_2(XylNC)_6]X_2$ (X = PF_6, BF_4) Yielding $[Pd_2(\mu\text{-dpmppm})(XylNC)_3](PF_6)_2$ ($[\mathbf{1}](PF_6)_2$) and $[Pd_2(\mu\text{-dpmppm})_2]X_2$ ($[\mathbf{2}]X_2$, X = PF_6, BF_4)

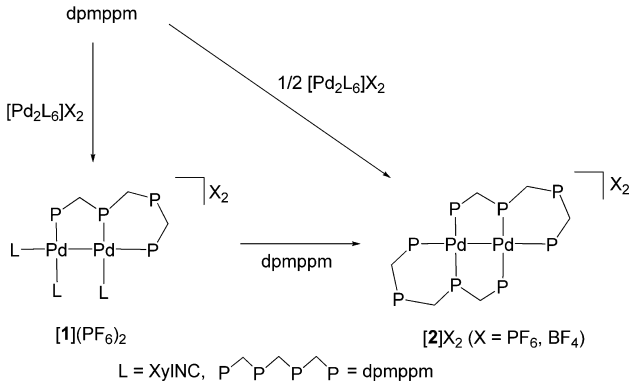

mass spectra of $[\mathbf{2}]X_2$ in CH_2Cl_2 at room temperature exhibited divalent intense peaks assignable to $[Pd_2(dpmppm)_2]^{2+}$ (m/z = 735.082; see the Supporting Information (SI), Figures S1a,b). The UV−vis absorption spectra in CH_2Cl_2 showed a characteristic band at 458 nm which is assignable to $\sigma-\sigma^*$ transition of the Pd^I-Pd^I covalent bond.[13] The $^{31}P\{^1H\}$ NMR spectra were consistent with the solid state structures (*vide infra*), indicating the presence of uncoordinated P atoms at around δ −48 ppm (Figures S2a,b). When $[Pd_2(XylNC)_6](PF_6)_2$ was treated with 1 equiv of dpmppm, yellow dipalladium(I) complex, $[Pd_2(\mu\text{-dpmppm})(XylNC)_3](PF_6)_2$ $[\mathbf{1}](PF_6)_2$, was obtained in 56% yield and was transformed by treatment with another equivalent of dpmppm into $[\mathbf{2}](PF_6)_2$, quantitatively (Scheme 2). The IR spectrum showed three C≡N stretching vibrations at 2188, 2168, and 2158 cm^{-1}, and in the ^1H NMR spectrum two methyl signals were observed at δ 1.93 and 2.11 in a ratio of 2:1, indicating the presence of three terminal XylNC ligands. In the $^{31}P\{^1H\}$ NMR spectrum (Figure S2c), four distinct resonances were detected at δ −2.51 (P_B), −11.20 (P_A), −19.16 (P_D), and −39.23 ppm (P_C) (see Experimental Section for notation), suggesting that the dpmppm ligand adopts μ-κ^1:κ^2 mode as is determined in the X-ray crystal structure (*vide infra*). The ESI−MS also exhibited a cation peak corresponding to $[Pd_2(\mu\text{-dpmppm})(XylNC)_3]^{2+}$ at m/z = 617.66 (z = 2) (Figure S1c).

The detailed structures of $[\mathbf{1}](PF_6)_2$ and $[\mathbf{2}](PF_6)_2$ were determined by X-ray crystallography. Perspective drawings for the complex cations are illustrated in Figure 1 and Figure S3. The asymmetric unit of $[\mathbf{2}](PF_6)_2$ contains an independent dipalladium complex cation and two hexafluorophosphate anions together with dichloromethane solvent molecules. The structure consists of two Pd atoms supported by two dpmppm ligands, possessing a pseudo C_2 axis bisecting the Pd−Pd bond

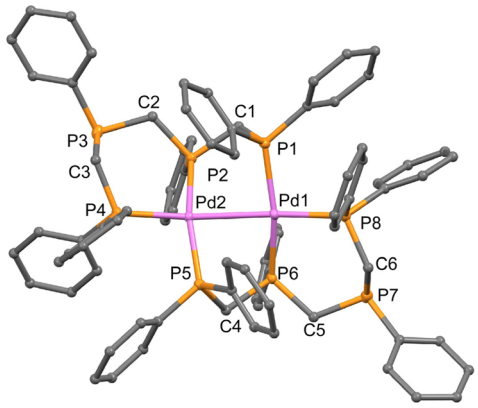

Figure 1. Perspective drawing for the complex cation of $[\mathbf{2}](PF_6)_2$. Selected bond distances (Å) and angles (deg): Pd1−Pd2 = 2.7379(5), Pd1−P1 = 2.3387(11), Pd1−P6 = 2.3057(11), Pd1−P8 = 2.3625(14), Pd2−P2 = 2.2975(12), Pd2−P4 = 2.3470(15), Pd2−P5 = 2.3306(12), Pd2−Pd1−P1 = 82.26(3), Pd2−Pd1−P6 = 86.70(3), Pd2−Pd1−P8 = 168.09(3), P1−Pd1−P6 = 161.96(4), P1−Pd1−P8 = 97.38(4), P6−Pd1−P8 = 95.53(4), Pd1−Pd2−P2 = 86.26(3), Pd1−Pd2−P4 = 164.72(3), Pd1−Pd2−P5 = 84.06(3), P2−Pd2−P4 = 97.48(5), P2−Pd2−P5 = 160.58(5), P4−Pd2−P5 = 96.26(5). The Pd and P atoms are illustrated with thermal ellipsoids at 40% probability level. The hydrogen atoms are omitted and the C atoms are drawn with arbitrary spherical model for clarity. Pd (violet), P (orange), and C (gray).

(Figure 1). The dipalladium(I) complexes with all the coordination sites occupied by phosphine units are relatively rare, examples being limited only to $[Pd_2(\mu\text{-etp})_2]^{2+}$ (etp = $Ph_2P(CH_2)_2PPh(CH_2)_2PPh(CH_2)_2PPh_2$),[14] $[Pd_2(PMe_3)_6]^{2+}$,[15] and $[Pd_2(\mu\text{-}Ph_2P(NH)PPh_2)_2(PPh_3)_2]^{2+}$.[16] The Pd−Pd distance of 2.7379(5) Å is within the range observed for usual Pd^I-Pd^I covalent bonds[13] but is significantly longer than that of the structurally resembled $[Pd_2(\mu\text{-etp})_2]^{2+}$ (2.617(2) Å).[14] The tetraphosphine bridges two Pd ions in asymmetrical μ-κ^1:κ^2 fashion forming conjugated $[Pd_2PCP]$ five- and $[PdPCPCP]$ six-membered rings. The dihedral angle of two square planes around the Pd atoms is 45.78(4)°, which is slightly larger than those for the palladium dimers with two PCP bridges of dppm ligands and is definitively smaller than that of $[Pd_2(\mu\text{-etp})_2]^{2+}$ (67°) with PCCP bridges.[14] The structure of $[\mathbf{1}](PF_6)_2$ also consists of two meta−metal bonded Pd(I) ions bridged by a μ-κ^1:κ^2−dpmppm ligand similar to $[\mathbf{2}](PF_6)_2$ together with three terminal isocyanide ligands (Figure S3). The overall structure of $[\mathbf{1}]^{2+}$ is quite similar to that observed in $[Pd_2(dpmppmF_2)(XlyNC)_3]^{2+}$ (Pd−Pd = 2.6122(5) Å)[12] and, however, the Pd−Pd bond length of $[\mathbf{1}]^{2+}$ (2.5702(2) Å) is appreciably shorter, implying that the electron-withdrawing 3,5-difluorophenyl groups have critical influence on the Pd−Pd bond.

The crystal structure of $[\mathbf{2}](PF_6)_2$ and its solution spectra demonstrated that the dipalladium(I) core is stabilized well by two μ-κ^1,κ^2-dpmppm ligands, even though the Pd−Pd bond is elongated to some extent (Pd−Pd = 2.7379(5) Å), which is interestingly contrasted to the Pd^I_2 structure of $[Pd_2(\mu\text{-}dpmppmF_2)_2(XylNC)_2]^{2+}$ ($[\mathbf{2F}]^{2+}$) possessing noncoordinated terminal phosphine pendants (Pd−Pd = 2.6892(4) Å).[12] The cyclic voltammogram (CV) of $[\mathbf{2}](PF_6)_2$ in acetonitrile notably showed a reversible reduction wave at $E_{1/2}$ = −1.07 V (vs Ag/$AgPF_6$) with ΔE = 69 mV (Figure S4). A coulometric analysis at −1.2 V consumed ca. 2 F per mole of $[\mathbf{2}]^{2+}$ and revealed that the reversible wave corresponds to a two-electron reduction process, $[Pd_2(\mu\text{-dpmppm})_2]^{2+} + 2e^- \rightleftarrows [Pd_2(\mu\text{-dpmppm})_2]^0$.

DOI: 10.1021/acs.inorgchem.5b00950
Inorg. Chem. 2015, 54, 8298−8309

Scheme 3. Reactions of $[2](PF_6)_2$ with $[Pd(dba)_2]$ (2 equiv) and Isocyanide (3 equiv)

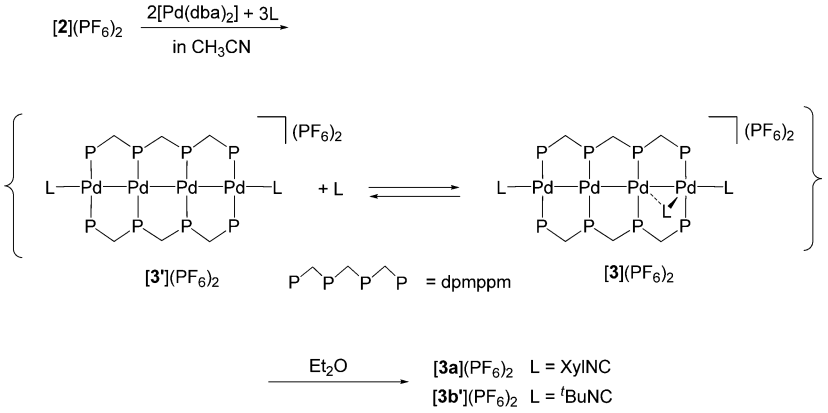

Synthesis of Tetrapalladium Complexes, $[Pd_4(\mu\text{-dpmppm})_2(L)_n](PF_6)_2$ (n = 2 ($[3'](PF_6)_2$), 3 ($[3](PF_6)_2$) from $[2](PF_6)_2$ (L = XylNC, ^{t}BuNC). When $[2](PF_6)_2$ was reacted with 2 equiv of $[Pd(dba)_2]$ in the presence of XylNC (3 equiv), or $[Pd_3(XylNC)_6]$ (2/3 equiv) at 60 °C for 5 h, the color of the solution immediately changed to bluish green and then to deep green, from which a green powder formulated as $[Pd_4(\mu\text{-dpmppm})_2(XylNC)_3](PF_6)_2$ ($[3a](PF_6)_2$) was obtained in 33% yield (Scheme 3). The IR spectrum showed three C≡N stretching bands at 2130, 2098, and 2040 cm^{-1}, suggesting the presence of three nonequivalent terminal isocyanide ligands. Complex $[3a](PF_6)_2$ was stable in acetonitrile but gradually decomposed in dichloromethane even under an inert atmosphere. The $^1H\{^{31}P\}$ and $^{31}P\{^1H\}$ NMR spectra in CD_3CN were rather broad at 20 °C, suggesting fluxional behaviors (Figure 2a, Figure S5). The UV−vis spectra

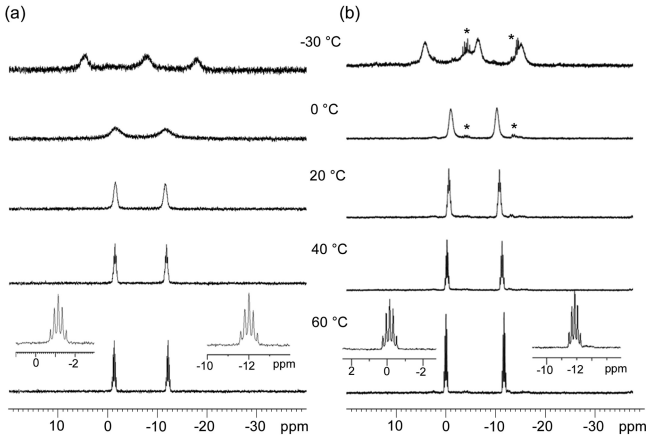

Figure 2. Variable temperature $^{31}P\{^1H\}$ NMR spectra in CD_3CN of (a) $[Pd_4(\mu\text{-dpmppm})_2(XylNC)_3](PF_6)_2$ ($[3a](PF_6)_2$) and (b) $[Pd_4(\mu\text{-dpmppm})_2(^t BuNC)_2](PF_6)_2$ ($[3b'](PF_6)_2$) + ^{t}BuNC (1 equiv). Asterisk indicates impurity.

in CH_3CN showed a reversible temperature-dependent spectral change, where a band at 673 nm (20 °C) shifted to an absorption around 639 nm (−30 °C; Figure 3a). These spectral features are quite similar to those of $[Pd_4(\mu\text{-dpmppmF}_2)_2(RNC)_3](PF_6)_2$ ($[3F](PF_6)_2$, R = Xyl, ^{t}Bu, and 2,6-diisopropylphenyl (Dip)), which have been elucidated to be attributed to an equilibrium as shown in Scheme 1b.[12] A similar treatment of $[2](PF_6)_2$ in the presence of ^{t}BuNC (3 equiv) afforded a deep green solution, but the isolated powder was

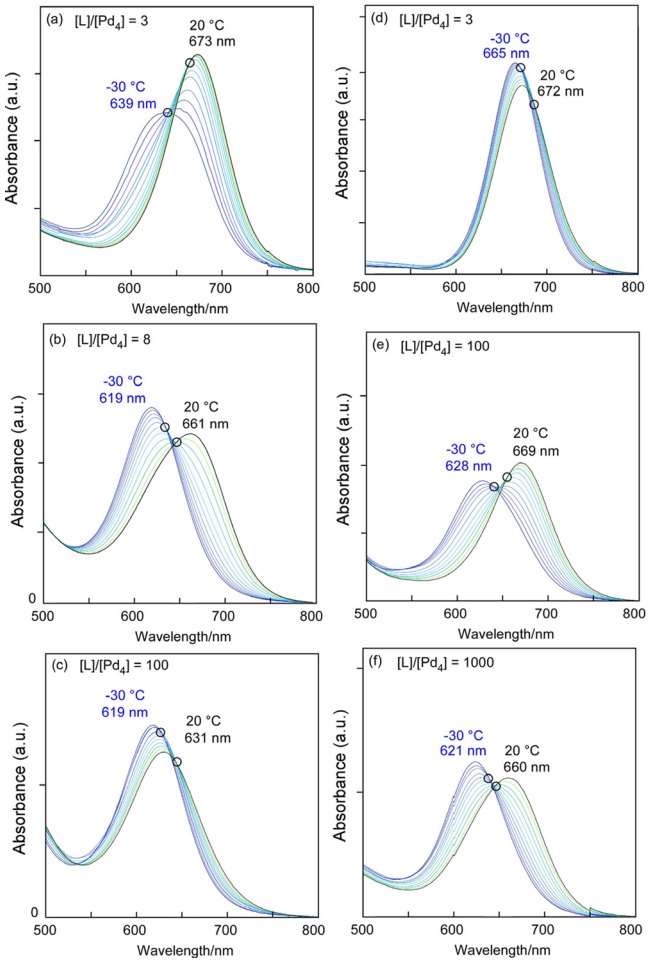

Figure 3. Variable-temperature UV−vis spectral changes (20 °C to −30 °C) in CH_3CN for solutions of $[Pd_4(\mu\text{-dpmppm})_2(XylNC)_3](PF_6)_2$ ($[3a](PF_6)_2$) with [L]/[Pd_4] ratios of (a) 3, (b) 8, and (c) 100 (L = XylNC) and those of $[Pd_4(\mu\text{-dpmppm})_2(^t BuNC)_2](PF_6)_2$ ($[3b'](PF_6)_2$) with [L]/[Pd_4] ratios of (d) 3, (e) 100, and (f) 1000 (L = ^{t}BuNC).

analyzed with a formula of $[Pd_4(\mu\text{-dpmppm})_2(^t BuNC)_2](PF_6)_2$ ($[3b'](PF_6)_2$), in which two isocyanide ligands are involved in the Pd_4 unit (Scheme 3). The IR spectrum exhibited only one C≡N peak at 2171 cm^{-1}. The $^{31}P\{^1H\}$ NMR spectrum at 20 °C in the presence of ^{t}BuNC (1 equiv; Figure 2b) showed two somewhat sharp signals at δ −10.9 and −0.7, still showing the

DOI: 10.1021/acs.inorgchem.5b00950
Inorg. Chem. 2015, 54, 8298−8309

dynamic behavior at a lower temperature around −30 °C. The UV−vis spectra in the presence of ^{t}BuNC (1 equiv) did not show the characteristic temperature-dependent blue shift at −30 °C as observed for the XylNC complex of $[\mathbf{3a}](PF_6)_2$ (Figure 3d). The ESI mass spectra of $[\mathbf{3a}](PF_6)_2$ and $[\mathbf{3b}'](PF_6)_2$ in the presence of free isocyanide showed dication peaks at m/z = 924.506 and 972.642, assignable to $[Pd_4(dpmppm)_2(RCN)_2]^{2+}$ (m/z = 924.560 (R = ^{t}Bu), 972.560 (R = Xyl)) (Figure S6). These results implied that the tetrapalladium complexes existed in the solution states with an equilibrium mixture as is observed for the solutions of $[Pd_4(\mu\text{-}dpmppmF_2)_2(RNC)_3](PF_6)_2$ ($[\mathbf{3F}](PF_6)_2$) which was dissociated into $[Pd_4(\mu\text{-}dpmppmF_2)_2(RNC)_2](PF_6)_2$ ($[\mathbf{3F}'](PF_6)_2$) and RNC at a higher temperature (Scheme 1b).[12] The solid-state structures of $[\mathbf{3F}](PF_6)_2$ (R = Xyl, ^{t}Bu) were unambiguously determined by X-ray crystallography, and the solution of $[\mathbf{3F}](PF_6)_2$ at low temperatures still exhibited fluxional behavior through exchanging terminal and bridging isocyanides.[12]

The variable temperature (VT) $^{31}P\{^1H\}$ NMR spectra of $[\mathbf{3a}](PF_6)_2$ were measured at −30 to 60 °C in CD_3CN (Figure 2a). At 60 °C, the $^{31}P\{^1H\}$ NMR spectrum showed two sharp quintet peaks of A_4B_4 spin system at δ −12.0 and −1.1 in a 1:1 ratio, which suggested that $[\mathbf{3a}](PF_6)_2$ adopted a symmetrical tetrapalladium structure, $[Pd_4(\mu\text{-}dpmppm)_2(XylNC)_2]^{2+}$ ($[\mathbf{3a}']^{2+}$), through dissociation of the bridging isocyanide ligand as shown in Scheme 3. When the temperature decreased below 20 °C to −30 °C, the ^{31}P peaks broadened, and then they split into three very broad signals around −18.1, −7.3, and 4.5 ppm, which resembled the $^{31}P\{^1H\}$ NMR spectra of $[\mathbf{3Fa}](PF_6)_2$ at 0 °C and $[\mathbf{3Fb}](PF_6)_2$ at −30 °C (Figure S7). The $^1H\{^{31}P\}$ NMR spectrum of $[\mathbf{3a}](PF_6)_2$ at 60 °C (Figures S5a,b) exhibited one singlet o-methyl signal at δ 1.82 and four doublets for the methylene protons of dpmppm ligands at δ 2.72, 3.77, 3.88, and 4.03 in a 1:2:1:2 ratio, which is in agreement with the symmetrical linear Pd_4 structure $[\mathbf{3a}'](PF_6)_2$. The VT $^{31}P\{^1H\}$ NMR features of $[\mathbf{3b}'](PF_6)_2$ in the presence of ^{t}BuNC (1 equiv; Figure 2b) were essentially similar to those of $[\mathbf{3a}](PF_6)_2$ (Figure 2a) and $[\mathbf{3Fb}](PF_6)_2$ (Figure S7b), in which two broad singlet peaks at δ −10.6 and −1.0 at 0 °C became well resolved at 60 °C into two quintets at δ = −11.9 and −0.1. At −30 °C, the peaks split into four very broad resonances around −15.3, −6.6 to −1.3, and 4.1 ppm. The $^1H\{^{31}P\}$ NMR spectrum (Figure S5c,d) at 60 °C exhibited one singlet methyl signal at δ 1.10 for ^{t}BuNC and four doublets of methylene protons at δ 2.52, 3.68, 3.79, and 4.03 in a 1:2:1:2 ratio, which also supported the symmetrical linear Pd_4 structure $[\mathbf{3b}'](PF_6)_2$.

To further elucidate the solution behaviors, temperature-dependent UV−vis spectra were measured for acetonitrile solutions including $[\mathbf{3a}](PF_6)_2$ and $[\mathbf{3b}'](PF_6)_2$ in the presence of a variable amount of RNC (3, 8, 100, 1000 equiv for $[Pd_4]^{2+}$). The UV−vis spectra with 3 equiv of XylNC exhibited temperature-dependent spectral changes, identical to those of $[\mathbf{3a}](PF_6)_2$, and showed a reversible temperature dependency with a band at 673 nm (20 °C) shifting to an absorption around 639 nm (−30 °C) through two isosbestic points (Figure 3a). In the presence of excess XylNC (8 equiv), a characteristic absorption band at 20 °C moved to around 661 nm, and with temperature decreasing, they shifted to a new band around 619 nm at −30 °C via another pair of isosbestic points (Figure 3b). With a large excess of XylNC (100 equiv), the low temperature absorption band reached its maximum at 619 nm (−30 °C; Figure 3c). These spectral differences reflect the equilibrium shift for $[\mathbf{3a}']^{2+} + L \rightleftarrows [\mathbf{3a}]^{2+}$ depending on the concentration of L. The UV−vis spectra in the presence of 3 equiv of ^{t}BuNC (Figure 3d) did not show the marked spectral changes as observed with XylNC, an absorption at 672 nm at 20 °C shifting slightly to 665 nm at −30 °C. However, in the presence of a larger excess of ^{t}BuNC (100 equiv), the band at 669 nm (20 °C) was converted to a higher energy band at 628 nm (−30 °C) via two isosbestic points (Figures 3e), and with 1000 equiv of ^{t}BuNC, an absorption at 660 nm at 20 °C shifted to 621 nm at −30 °C (Figure 3f), similar to a dynamic spectral changes as observed with 8 equiv of XylNC (Figure 3b). These spectral changes were essentially alike to those observed with $[Pd_4(\mu\text{-}dpmppmF_2)_2(RNC)_3](PF_6)_2$ (R = Xyl ($[\mathbf{3Fa}](PF_6)_2$), ^{t}Bu ($[\mathbf{3Fb}](PF_6)_2$)[12], and suggested that the tetrapalladium complexes $[\mathbf{3a}'](PF_6)_2$ and $[\mathbf{3b}'](PF_6)_2$ were equilibrated to $[\mathbf{3a}](PF_6)_2$ and $[\mathbf{3b}](PF_6)_2$, respectively, in the acetonitrile solution states as shown in Scheme 3. In addition, it should be noted that XylNC has much higher affinity to the linear Pd_4 core $\{Pd_4(\mu\text{-}dpmppm)_2(RNC)_2\}^{2+}$ than ^{t}BuNC on the basis of the UV−vis spectra.

In order to determine the binding constants K for $[\mathbf{3}']^{2+} + L \rightleftarrows [\mathbf{3}]^{2+}$, titrations of $[\mathbf{3a}](PF_6)_2$ and $[\mathbf{3b}'](PF_6)_2$ with successive addition of isocyanides, XylNC and ^{t}BuNC, were carried out at 20 °C by monitoring UV−vis spectra (Figure 4b

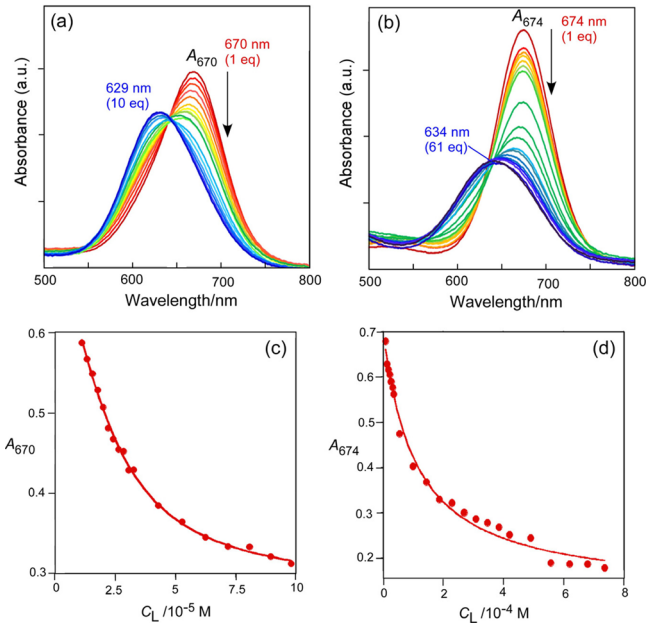

Figure 4. (a) UV−vis spectral changes of $[Pd_4(\mu\text{-}dpmppmF_2)_2(XylNC)_3](PF_6)_2$ ($[\mathbf{3Fa}](PF_6)_2$) in CH_3CN by successive titration of XylNC at 20 °C. (b) UV−vis spectral changes of $[Pd_4(\mu\text{-}dpmppm)_2(XylNC)_3](PF_6)_2$ ($[\mathbf{3a}](PF_6)_2$) in CH_3CN by successive titration of XylNC at 20 °C. (c) Plots of A_{670} vs concentration of XylNC (C_L) and the fitted line for $[\mathbf{3Fa}']^{2+} + L \rightleftarrows [\mathbf{3Fa}]^{2+}$. (d) Plots of A_{674} vs concentration of XylNC (C_L) and the fitted line for $[\mathbf{3a}']^{2+} + L \rightleftarrows [\mathbf{3a}]^{2+}$.

and Figure S8b). In addition, to assess the influence of the tetraphosphine ligands, $[\mathbf{3Fa}](PF_6)_2$ and $[\mathbf{3Fb}](PF_6)_2$ were also titrated with XylNC and ^{t}BuNC, respectively, at 20 °C (Figure 4a and Figure S8a). According to adding portions of XylNC to the solution including tetrapalladium complexes, the characteristic bands for $[\mathbf{3Fa}']^{2+}$ and $[\mathbf{3a}']^{2+}$ around 670 nm

DOI: 10.1021/acs.inorgchem.5b00950
Inorg. Chem. 2015, 54, 8298−8309

gradually decreased (Figures 4a,b), and plots of $A_{670/674}$ vs [XylNC] were subject to curve-fitting analysis with parameters K, $\varepsilon([\mathbf{3}']^{2+})$, $\varepsilon([\mathbf{3}]^{2+})$, and c_0 of $[\mathbf{3}']^{2+}$ or $[\mathbf{3F}']^{2+}$ (Figures 4c,d and Table S3). A similar procedure was also applied to titration of $[\mathbf{3b}']^{2+}$ and $[\mathbf{3Fb}']^{2+}$ with ^{t}BuNC (Figures S8a,b). At first, the binding constant of $[\mathbf{3Fa}']^{2+}$ with XylNC, 1.2×10^5 M^{-1}, is 10-fold larger than that of $[\mathbf{3a}']^{2+}$ with XylNC, 1.0×10^4 M^{-1}, which is ascribable to the electron deficient Pd_4 core of $[\mathbf{3Fa}']^{2+}$ due to the electron withdrawing 3,5-$F_2C_6H_3$ groups of dpmppmF_2 ligands. Whereas reliability of the curve-fitting with ^{t}BuNC was relatively low due to its smaller binding constants (Figures S8c,d), the obtained value of $[\mathbf{3Fb}']^{2+}$ with ^{t}BuNC, 7.3×10^2 M^{-1}, is larger than that of $[\mathbf{3b}']^{2+}$ with ^{t}BuNC of 3.9×10^2 M^{-1}, as is found for XylNC association, and notably both values are significantly smaller in comparison with those with XylNC, probably due to stronger σ-donating ability and larger steric bulkiness of ^{t}BuNC. The obtained K values in an order of $[\mathbf{3Fa}']^{2+} > [\mathbf{3a}']^{2+} \gg [\mathbf{3Fb}']^{2+} > [\mathbf{3b}']^{2+}$ are consistent with the temperature-dependent UV−vis spectral changes as described above.

Synthesis of Octapalladium Complexes, $[Pd_8(\mu\text{-dpmppm})_2(CH_3CN)_2]X_4$ from $[\mathbf{2}]X_2$ (X = PF_6, BF_4). When $[\mathbf{2}]X_2$ was reacted with 2 equiv of $[Pd(dba)_2]$ in acetonitrile at 60 °C for 3 h, the color of the solution changed to greenish brown, and crystallization of the acetonitrile solution by addition of diethyl ether precipitated greenish brown powders of $[Pd_8(\mu\text{-dpmppm})_4(CH_3CN)_2]X_4$ ($[\mathbf{4}]X_4$) in yields of 54% (X = BF_4)[11] and 58% (X = PF_6) determined by $^{31}P\{^1H\}$ NMR spectra (Scheme 4). Recrystallization of the powders from

Scheme 4. Preparation of Octapalladium Complexes $[\mathbf{4}]X_4$ from $[\mathbf{2}]X_2$ (X = PF_6, BF_4)

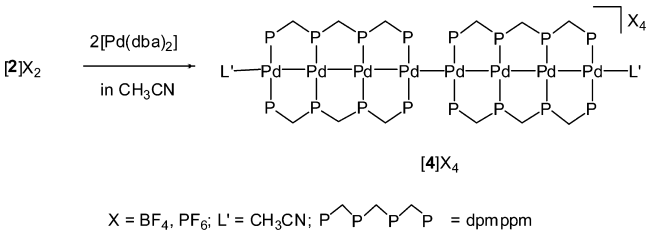

CH_3CN/Et_2O solutions afforded pale greenish brown single crystals in low isolated yields (8−13%), which were analyzed by IR, UV−vis−NIR absorption, ESI mass and $^1H\{^{31}P\}$ and $^{31}P\{^1H\}$ NMR spectroscopy (Figures S9−S11), and elemental analysis for $[\mathbf{4}](PF_6)_4$.

The $^{31}P\{^1H\}$ NMR spectrum of $[\mathbf{4}](PF_6)_4$ in CD_3CN at room temperature (Figure S11a) displayed a set of four multiplets at δ 2.5, −6.1, −9.0, and −15.6 ppm in a ratio of 1:1:1:1, which are diagnostic for the octapalladium structure, alongside a septet of PF_6 anion at −144.3 ppm. The $^1H\{^{31}P\}$ NMR spectra of $[\mathbf{4}](PF_6)_4$ (Figure S11b) exhibited the characteristic lower field-shifted doublets at 1.02 and 0.85 ppm, which correspond to the methylene protons of dpmppm ligands due to ring current effects of the C−H/π interactions as observed in the crystal structure of $[\mathbf{4}](BF_4)_4$.[11] The VT UV−vis−NIR spectral changes for an acetonitrile solution of $[\mathbf{4}](PF_6)_4$ are depicted in Figure S9, featuring thermochromics behavior with an intense absorption of 896 nm at −30 °C. The spectroscopic features of $[\mathbf{4}](PF_6)_4$ are almost identical to those of $[\mathbf{4}](BF_4)_4$, indicating that the counteranions have no influence on the Pd_8 structure. The present results revealed that $[\mathbf{2}]X_2$ was a viable precursor of Pd chains, which were extended to octanuclear in acetonitrile and, in contrast, terminated at tetranuclear in the presence of isocyanides.

Synthesis of Pd_2M_2 Complexes, $[Pd_2Cl(Cp^*MCl)(Cp^*MCl_2)(\mu\text{-dpmppm})_2](PF_6)_2$ from $[\mathbf{2}](PF_6)_2$ (M = Rh, Ir). Reaction of $[\mathbf{2}](PF_6)_2$ with 1 equiv of $[Cp^*MCl_2]_2$ (M = Rh, Ir) in dichloromethane at room temperature gave mixed-metal tetranuclear complexes, $[Pd_2Cl(Cp^*MCl)(Cp^*MCl_2)(\mu\text{-dpmppm})_2](PF_6)_2$, in yields of 47% (M = Rh ($[\mathbf{5}](PF_6)_2$) and 52% (M = Ir ($[\mathbf{6}](PF_6)_2$; Scheme 5). The structures were

Scheme 5. Preparation of Pd_2M_2 Complexes, $[Pd_2Cl(Cp^*MCl)(Cp^*MCl_2)(\mu\text{-dpmppm})_2](PF_6)_2$ from $[\mathbf{2}](PF_6)_2$ (M = Rh ($[\mathbf{5}](PF_6)_2$), Ir ($[\mathbf{6}](PF_6)_2$))

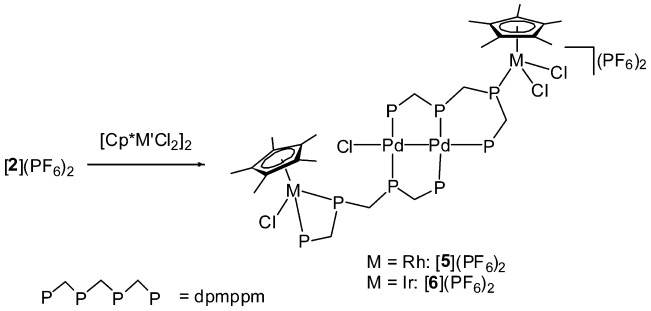

determined by X-ray crystallography; perspective views are illustrated in Figure 5 and Figure S12. The structures of $[\mathbf{5}](PF_6)_2$ and $[\mathbf{6}](PF_6)_2$ are isomorphous to each other and contain a metal−metal bonded asymmetric dipalladium(I) core of $\{Pd_2Cl(\mu\text{-dpmppm})_2\}^+$ (Pd1−Pd2 = 2.6932(6) Å ($[\mathbf{5}]^{2+}$), 2.710(2) Å ($[\mathbf{6}]^{2+}$); Pd2−Cl4 = 2.441(2) Å ($[\mathbf{5}]^{2+}$), 2.468(7) Å ($[\mathbf{6}]^{2+}$)). One dpmppm ligand supports the Pd_2 unit in μ-κ^1;κ^2 fashion as in $[\mathbf{2}]^{2+}$, and the noncoordinate P atom involved in the [PdPCPCP] ring of $[\mathbf{2}]^{2+}$ ligates to $\{Cp^*MCl_2\}$ unit, resulting in a μ-κ^1;κ^2; κ^1 bridging structure for Pd2Pd1M1 centers. Owing to the coordination of the $\{Cp^*MCl_2\}$ unit, the stable chair conformation of the [PdPCPCP] ring in $[\mathbf{2}]^{2+}$ was deformed to a highly distorted twist boat form to avoid steric repulsions (P1−Pd1−P3 = 91.48(6)° ($[\mathbf{5}]^{2+}$), 92.4(2)° ($[\mathbf{6}]^{2+}$)). Similar conformational change was observed in the mononuclear Pd complex, $[PdCl(dpmppm\text{-}\kappa^3)]^+$ forming $[PdCl(Cp^*MCl_2)(\mu\text{-dpmppm-}\kappa^1,\kappa^3)]^{2+}$ (M = Rh, Ir) adducts.[9f] The other dpmppm also bridges the Pd_2 core with μ-κ^1;κ^1 mode of outer and inner neighboring P atoms, and the other pair of P atoms makes a four-membered chelate ring to the $\{Cp^*MCl\}$ fragment (P7−M2−P8 = 72.40(7)° ($[\mathbf{5}]^{2+}$), 70.89(19)° ($[\mathbf{6}]^{2+}$)), leading to a μ-κ^1;κ^1;κ^2 structure for Pd1Pd2M2 centers. The M1···Pd1 distances are 6.3240(7) Å ($[\mathbf{5}]^{2+}$) and 6.454(2) Å ($[\mathbf{6}]^{2+}$), and the M2···Pd2 distances are 7.0042(7) Å ($[\mathbf{5}]^{2+}$) and 6.938(2) Å ($[\mathbf{6}]^{2+}$), all being out of range for the metal−metal interaction.

The solution structures of $[\mathbf{5}]^{2+}$ and $[\mathbf{6}]^{2+}$ were analyzed by ESI−MS and ^1H and $^{31}P\{^1H\}$ NMR spectra to reveal that the asymmetric Pd_2M_2 crystal structures were retained in dichloromethane solutions. The ESI mass spectra in CH_2Cl_2 showed monovalent cation peaks at m/z = 2231.665 ($[\mathbf{5}](PF_6)_2$) and 2411.942 ($[\mathbf{6}](PF_6)_2$), corresponding to $\{Pd_2Cl(Cp^*MCl)(Cp^*MCl_2)(\mu\text{-dpmppm})_2](PF_6)\}^+$ (2232.040 (M = Rh) and 2411.161 (M = Ir) (Figure S13). The characteristic UV−vis absorption band typical for a Pd^I−Pd^I bond was observed at 464−465 nm, slightly red-shifted in comparison with 458 nm of $[\mathbf{2}]X_2$.

DOI: 10.1021/acs.inorgchem.5b00950
Inorg. Chem. 2015, 54, 8298−8309

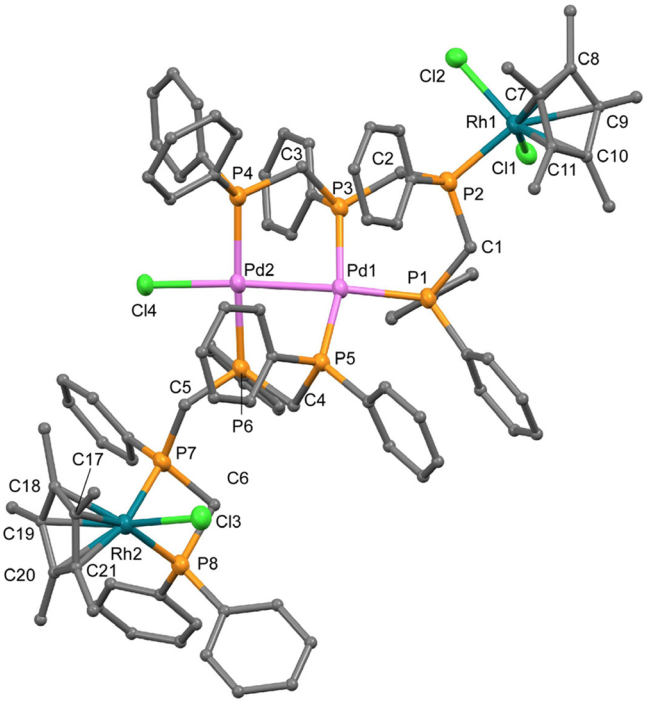

Figure 5. Perspective drawing for the complex cation of $[\mathbf{5}](PF_6)_2$. Selected bond distances (Å) and angles (deg): Pd1−Pd2 = 2.6932(3), Pd1−P1 = 2.379(2), Pd1−P5 = 2.327(2), Pd2−Cl4 = 2.441(2), Pd2−P4 = 2.333(2), Pd2−P6 = 2.341(2), Rh1−Cl1 = 2.427(2), Rh1−Cl2 = 2.431(2), Rh1−P2 = 2.324(2), Rh2−Cl3 = 2.425(2), Rh2−P7 = 2.340(2), Rh2−P8 = 2.336(2), Pd2−Pd1−P1 = 165.68(5), Pd1−Pd2−Cl4 = 176.12(5), P1−Pd1−P3 = 91.48(6), P7−Rh2−P8 = 72.40(7). The Pd, Rh, Cl, and P atoms are illustrated with thermal ellipsoids at the 40% probability level. The hydrogen atoms are omitted, and the C atoms are drawn with an arbitrary spherical model for clarity. Pd (violet), Rh (blue), Cl (green), P (orange), and C (gray).

In the ^{1}H NMR spectra of $[\mathbf{5}]^{2+}$ and $[\mathbf{6}]^{2+}$ in CD_2Cl_2, methyl signals of the two Cp* groups were observed as a doublet (δ 1.42 with $^4J_{PH}$ = 4.0 Hz for $[\mathbf{5}]^{2+}$, δ 1.30 with $^4J_{PH}$ = 2.5 Hz for $[\mathbf{6}]^{2+}$) and a triplet (δ 1.49 with $^4J_{PH}$ = 3.9 Hz for $[\mathbf{5}]^{2+}$, δ 1.50 with $^4J_{PH}$ = 2.6 Hz for $[\mathbf{6}]^{2+}$) in a 1:1 ratio. The $^{31}P\{^1H\}$ NMR spectra were assigned by using $^{31}P-^{31}P$ COSY techniques as a $P_{A1}P_{A2}P_{B1}P_{B2}P_{C1}P_{C2}P_{D1}P_{D2}$ system (see Experimental Section, Figure S14). In the spectrum of $[\mathbf{5}]^{2+}$, the peaks for P_{C1} attached to the $\{Cp^*RhCl_2\}$ unit were observed at δ 20.1 ppm with $^1J_{RhP}$ = 149 Hz, and those for P_{C2} and P_{D2} chelating to the $\{Cp^*RhCl\}$ center appeared at δ −10.7 and 1.9 ppm with $^1J_{RhP}$ = 109 and 114 Hz. On the other hand, for $[\mathbf{6}]^{2+}$, the signal of P_{C1} was observed at δ −11.2 ppm, and those of P_{C2} and P_{D2} significantly shifted toward lower field at −29.4 and −48.6 ppm due to four-membered chelation to the Ir center. The resonances of P_{A1}, P_{A2}, P_{B1}, and P_{B2} showed large *trans*-P,P′ coupling across the square planar Pd centers.

Although attempts to identify intermediate species by monitoring $^{31}P\{^1H\}$ NMR spectra at low temperatures were not successful yet, a plausible intermediate of the symmetric Pd_2M_2 complex, $[Pd_2(Cp^*MCl_2)_2(\mu\text{-dpmppm})_2](PF_6)_2$ (**I**), could be postulated on the basis of reactions of the mononuclear Pd^{II} complex, $[PdCl(dpmppm\text{-}\kappa^3)]^+$, with $[Cp^*MCl_2]_2$,[9f] and the intermediate (**I**) was estimated to be very unstable and readily converted into the asymmetric structure of $[\mathbf{5}]^{2+}$ and $[\mathbf{6}]^{2+}$ to release strains accumulated in the two $\{Cp^*MCl_2\}$ fragment-attached six-membered [PdPCPCP] rings (Scheme 6). In particular, the axial phenyl groups on the P_C atom are estimated to cause significant repulsive interactions between the phenyl groups around the Pd−Pd bond in **I**.

Scheme 6

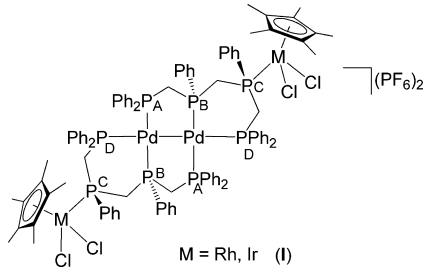

Synthesis of Au_2Pd_2 Complexes, $[Au_2Pd_2Cl_2(dpmppm-H)_2](PF_6)_2$ ($[\mathbf{7}](PF_6)_2$) from $[\mathbf{2}](PF_6)_2$. When $[\mathbf{2}](PF_6)_2$ was treated with 2 equiv of $[AuCl(PPh_3)]$ in dichloromethane at room temperature, yellow crystals of a Au_2Pd_2 mixed-metal complex, $[Au_2Pd_2Cl_2(dpmppm-H)_2](PF_6)_2$ ($[\mathbf{7}](PF_6)_2$) were isolated in a low yield of 7% (Scheme 7). The ESI−MS in CH_2Cl_2 exhibited two sets of intense peaks

Scheme 7. Preparation of Au_2Pd_2 Complexes, $[Au_2Pd_2Cl_2(dpmppm-H)_2](PF_6)_2$ ($[\mathbf{7}](PF_6)_2$) from $[\mathbf{2}](PF_6)_2$

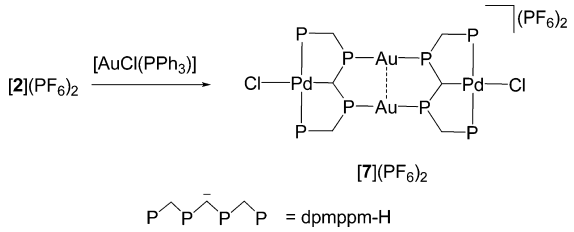

at m/z = 966.038 (z = 2) and 2077.061 (z = 1), corresponding to $[Au_2Pd_2Cl_2(dpmppm-H)_2]^{2+}$ (966.009) and $\{[Au_2Pd_2Cl_2(dpmppm-H)_2](PF_6)\}^+$ (2076.982) (Figure S15). The $^1H\{^{31}P\}$ NMR spectrum in CD_2Cl_2 indicated very simple methylene signals with two doublets at δ 3.40 and 3.97 ($^2J_{HH}$ = 15 Hz) and one singlet at δ 4.85 in a 2:2:1 ratio (Figure S16a), demonstrating a symmetrical coordination pattern of dpmppm ligand with a loss of one central methylene proton. In the $^{31}P\{^1H\}$ NMR spectrum, two multiplets were observed at δ 11.1 and 44.6 in a 1:1 ratio (Figure S16b). In the light of chemical shifts for Au−dpmppm complexes,[9] the higher field peak at 44.6 ppm could be assigned to the Au-bound P atoms.

The detailed structure of $[\mathbf{7}](PF_6)_2$ was determined by X-ray crystallography to comprise two [PdCl(dpmppm−H)] moieties connected by two Au^I ions through linear P−Au−P geometry, resulting in a crystallographically imposed C_i symmetry (Au1−P2 = 2.330(2) Å, Au1−P3* = 2.329(2) Å, P2−Au−P3* = 178.13(7)°) (Figures 6 and S17). The Au1···Au1* and Au1···Pd1 distances of 3.0902(9) Å and 3.796(1) Å indicate no metal−metal bonding interaction, while the former falls within the range of a weak aurophilic interaction.[17] The Pd1 atom is coordinated by a chloride ion and a PCP pincer ligand (dpmppm−H) derived from deprotonation of dpmppm to complete a pseudo C_s symmetrical square planar structure.

DOI: 10.1021/acs.inorgchem.5b00950
Inorg. Chem. 2015, 54, 8298−8309

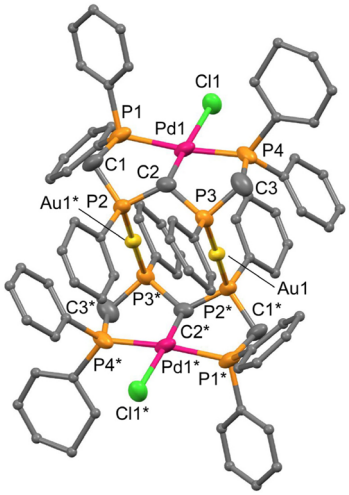

Figure 6. Perspective drawing for the complex cation of $[7](PF_6)_2$. Selected bond distances (Å) and angles (deg): Au1−P2 = 2.330(2), Au1−P3* = 2.329(2), Pd1−Cl1 = 2.360(8), Pd1−P1 = 2.327(3), Pd1−P4 = 2.313(3), Pd1−C2 = 2.096(11), P2−Au1−P3* = 178.13(7), Cl1−Pd1−P1 = 98.19(19), Cl1−Pd1−P4 = 83.92(18), Cl1−Pd1−C2 = 169.5(2), P1−Pd1−P4 = 167.71(10), P1−Pd1−C2 = 87.5(2), P4−Pd1−C2 = 88.7(2). The Au, Pd, Cl, P, and C atoms are illustrated with thermal ellipsoids at 40% probability level. The hydrogen atoms are omitted, and the C atoms of phenyl groups are drawn with an arbitrary spherical model for clarity. The disordered phenyl groups and Cl atoms are omitted for clarity. Pd (violet), Au (yellow), Cl (green), P (orange), and C (gray).

Although serious disorder of three phenyl groups of the PCP ligand and the Cl atom prevented further precise discussion on the crystal structure, the metalated C2 atom notably takes an sp^3 configuration with Pd1−C2−P2 = 107.3(4)°, Pd1−C2−P3 = 106.9(6)°, and P2−C2−P3 = 113.5(4)°. The Pd complexes with PC(sp^3)P pincer ligands are relatively limited compared with those with PC(sp^2)P ones,[18] and in addition, the PC(sp^3)P with a PCPCPCP backbone is unprecedented, though the carbodiphosphorane PCP pincer ligand of $C(dppm)_2$ (dppm = bis(diphenylphsophino)methane) has been reported by Schuh et al., which stabilized square planar complexes of Pt, Pd, and Ni through the neutral carbon (av. Pd−C = 2.057 Å, Pt−C = 2.060(4) Å).[19] The $C(dppm)_2$ is protonated to form $[CH(dppm)_2]Cl$, which also pinches Pt^{II} and Pd^{II} ions through the cationic central sp^3 carbon atom (Pd−C = 2.102(3) Å, Pt−C = 2.106(4) Å).[19] In contrast, the central sp^3 carbon of $[7](PF_6)_2$ is anionic, and the Pd−C bond length is 2.096(11) Å, which is comparable to that of $[PdCl(CH(CH_2CH_2PPh_2)_2)]$ (2.111 Å).[20]

CONCLUSION

In the present study, the metal−metal bonded binuclear Pd^I complexes, $[Pd_2(dpmppm)_2]X_2$ (X = PF_6, BF_4), were prepared by using a linear tetraphosphine, *meso*-bis[(diphenylphosphinomethyl)phenylphosphino]methane (dpmppm) and were proven useful precursors to extend palladium chains to $[Pd_4(\mu\text{-}dpmppm)_2(RNC)_2]^{2+}$ and $[Pd_8(\mu\text{-}dpmppm)_4(CH_3CN)_2]^{4+}$. By treating the Pd_2 complex with 2 equiv of $[Pd(dba)_2]$ in CH_3CN, the Pd chain is terminated in the presence of isocyanide ligands at the Pd_4 array of $[Pd_4(\mu\text{-}dpmppm)_2(RNC)_2]^{2+}$ (R = Xyl, ^{t}Bu), which are equilibrated to $[Pd_4(\mu\text{-}dpmppm)_2(RNC)_3]^{2+}$ in the presence of free isocyanide at low temperatures. In the absence of the isocyanides, two Pd_4 units are further connected to form an octanuclear palladium chain terminated by acetonitrile, $[Pd_8(\mu\text{-}dpmppm)_4(CH_3CN)_2]^{4+}$, which were assigned by VT $^{31}P\{^1H\}$ NMR spectra and temperature-dependent thermochromics behaviors. Furthermore, reactions of the Pd_2 complex with $[Cp^*MCl_2]_2$ (M = Rh, Ir) and $[AuCl(PPh_3)]$ afforded Pd_2M_2 heterometallic tetranuclear complexes, $[Pd_2Cl(Cp^*MCl)(Cp^*MCl_2)(\mu\text{-}dpmppm)_2](PF_6)_2$ (M = Rh, Ir) and $[Au_2Pd_2Cl_2(dpmppm{-}H)_2](PF_6)_2$, respectively. In the latter Au_2Pd_2 complex, a deprotonated dpmppm (dpmppm−H) acted as a novel PC(sp^3)P pincer ligand with a PCPCPCP backbone. These results demonstrate that the binuclear palladium(I) complexes with two dpmppm ligands are a viable precursor to developing low-valent palladium chains and Pd-involved mixed-metal multinuclear systems in stepwise procedures.

EXPERIMENTAL SECTION

General Procedures. All preparative procedures were carried out under a nitrogen atmosphere in a glovebox or using standard Schlenk techniques. Reagent grade solvents were dried by the standard procedures and were freshly distilled prior to their use. Compounds dpmppm,[9a] $[Pd(dba)_2]$ (dba = dibenzylideneacetone),[21] $[Pd_3(XylNC)_6]$,[22] $[Cp^*MCl_2]_2$ (M = Rh, Ir; Cp* = pentamethylcyclopentadienyl),[23] $[AuCl(PPh_3)]$,[24] $[Pd_2(XylNC)_6]X_2$ (X = PF_6, BF_4),[25] and $[Pd_4(\mu\text{-}dpmppmF_2)_2(RNC)_3](PF_6)_2$ ($[\mathbf{3F}](PF_6)_2$, R = Xyl, ^{t}Bu)[12] were prepared by the methods described in the literature. ^1H and $^1H\{^{31}P\}$ NMR spectra were recorded on a JEOL JNM-AL400 spectrometer (400 MHz) and Bruker AV-300N or Varian Gemini2000 instrument (300 MHz), and the frequencies were referenced to the residual resonances of the deuterated solvent. $^{31}P\{^1H\}$ NMR spectra were recorded on the same instrument at 162 and 121 MHz with chemical shifts being calibrated to 85% H_3PO_4 as an external reference. Electronic absorption spectra were recorded on Shimadzu UV-3100, Hewlett-Packard Agilent 8453, and Jasco UV600 spectrophotometers at various temperatures. IR spectra of solid compounds as KBr disks were recorded on a Jasco FT/IR-410 spectrophotometer at ambient temperature. ESI−TOF mass spectra were recorded on a JEOL JMS-T100LC in a positive detection mode in the range of m/z 100−3000, equipped with an ion spray interface. Electrochemical measurements were performed with a Hokuto-Denko HZ-3000 system. $[^nBu_4N][PF_6]$ was used as a supporting electrolyte, which was recrystallized from ethanol before use. Cyclic voltammetry experiments were carried out with 2 mM acetonitrile solutions of the samples containing 0.1 M $[^nBu_4N][PF_6]$, by using a standard three-electrode cell consisting of a $Ag/AgPF_6$ reference electrode, platinum wire as a counter-electrode, and a glassy carbon electrode as a working electrode.

Preparation of $[Pd_2(\mu\text{-}dpmppm)(XylNC)_3](PF_6)_2$ ($[\mathbf{1}](PF_6)_2$). To a solution of $[Pd_2(XylNC)_6](PF_6)_2$ (101 mg, 78 μmol) in CH_2Cl_2 (10 mL) was added dpmppm (55 mg, 88 μmol), and the solution was stirred for 3 h at room temperature. The color of the solution turned from yellow to red and to yellow. The solvent was removed under reduced pressure to dryness, and the residue was washed with Et_2O and extracted with CH_2Cl_2 (5 mL). The extract was filtered and concentrated to ca. 3 mL. After careful addition of Et_2O (1 mL), the solution was allowed to stand at room temperature to afford yellow block crystals of $[\mathbf{1}](PF_6)_2{\cdot}0.5CH_2Cl_2$, which were filtered off, washed with Et_2O, and dried in vacuo. Yield: 68 mg, 56% (vs Pd). ^1H NMR (300 MHz, CD_2Cl_2, r.t.): δ 1.93 (s, 12H, CH_3), 2.11 (s, 6H, CH_3), 2.54−2.91 (m, br, 4H, CH_2), 4.74 (m, br, 1H, CH_2), 5.16 (m, br, 1H, CH_2), 6.96−8.20 (m, 45H, Ar*H*). $^{31}P\{^1H\}$ NMR (121 MHz, CD_2Cl_2, r.t.): δ −144.9 (sep, $^1J_{PF}$ = 712 Hz, 2P, PF_6), −39.23 (dd, $J_{PP'}$ = 97, 80 Hz, 1P, P_C), −19.16 (dd, $J_{PP'}$ = 92, 37 Hz, 1P, P_D), −11.20 (d, $J_{PP'}$ = 56 Hz, 1P, P_A), −2.51 (ddd, $J_{PP'}$ = 80, 56, 39 Hz, 1P, P_B). ESI−MS (in CH_2Cl_2): m/z 617.657 (z = 2, $[Pd_2(dpmppm)(XylNC)_3]^{2+}$ (617.603)), 1380.273 (z = 1, $\{[Pd_2(dpmppm)(XylNC)_3]PF_6\}^+$

DOI: 10.1021/acs.inorgchem.5b00950
Inorg. Chem. 2015, 54, 8298−8309

(1380.171)). IR (KBr): ν 2188, 2168, 2158 (s, N≡C), 1436 (s, P−C), 1102 (s), 837 (vs, PF_6), 709 (w), 521 (s), 506 (s) cm^{-1}. UV−vis (CH_2Cl_2, r.t.): λ_{max} (log ε) 393 (4.45) nm. Anal. Calcd for $C_{66.5}H_{64}N_3ClF_{12}P_6Pd_2$ ([**2**]$(PF_6)_2$·0.5CH_2Cl_2): C, 50.96; H, 4.12; N, 2.68%. Found: C, 50.79; H, 4.02; N, 2.70%.

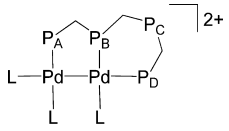

Preparations of [Pd_2(μ-dpmppm)$_2$]X_2 ([2]X_2, X = PF_6, BF_4). To a solution of [Pd_2(XylNC)$_6$]$(PF_6)_2$ (201 mg, 156 μmol) in CH_2Cl_2 (10 mL) was added dpmppm (220 mg, 351 μmol), and the solution was stirred for 2 h at room temperature. The color of the solution turned from yellow to orange. The solvent was removed under reduced pressure to dryness, and the residue was washed with Et_2O (2 mL × 5) and extracted with CH_2Cl_2 (4 mL). The extract was filtered and, after careful addition of Et_2O (3 mL), the solution was allowed to stand at room temperature to afford orange prismatic crystals of [**2**]$(PF_6)_2$·CH_2Cl_2, which were filtered off, washed with Et_2O, and dried in vacuo. Yield: 153 mg, 53% (vs Pd). ^{1}H NMR (300 MHz, CD_2Cl_2, r.t.): δ 1.37 (d, 2H, CH_2, J = 14 Hz), 1.56 (t, 2H, CH_2, J = 15 Hz), 2.17 (br, 2H, CH_2), 2.43 (br, 2H, CH_2), 4.25 (br, 2H, CH_2), 4.95 (br, 2H, CH_2), 6.65−8.24 (m, 60H, ArH). ^{31}P{^{1}H} NMR (121 MHz, CD_2Cl_2, r.t.): δ −144.7 (sep, $^1J_{PF}$ = 702 Hz, 2P, PF_6), −48.0 (m, 2P), −11.8 to −6.3 (m, 4P), −4.3 (m, 2P). ESI−MS (in CH_2Cl_2): m/z 735.118 (z = 2, [Pd_2(dpmppm)$_2$]$^{2+}$ (735.082)), 1615.244 (z = 1, {[Pd_2(dpmppm)$_2$]PF_6}$^+$ (1615.128)). IR (KBr): ν 1436 (s, P−C), 1139 (w), 1095 (m), 839 (vs, PF_6), 742 (s), 694 (s), 557 (s), 511 (m), 483 (m) cm^{-1}. UV−vis (CH_2Cl_2, r.t.): λ_{max} (log ε) 458 (4.36), 328 (4.01) nm. Anal. Calcd for $C_{79}H_{74}Cl_2F_{12}P_{10}Pd_2$ ([**2**]$(PF_6)_2$·CH_2Cl_2): C, 51.43; H, 4.04%. Found: C, 51.03; H, 4.00%.

By a procedure similar to that of [**2**]$(PF_6)_2$, using [Pd_2(XylNC)$_6$]$(BF_4)_2$ (242 mg, 206 μmol), [**2**]$(BF_4)_2$·0.5CH_2Cl_2 was isolated in 71% yield (241 mg). ^{1}H NMR (300 MHz, CD_2Cl_2, r.t.): δ 1.40 (d, 2H, CH_2, J = 14 Hz), 1.66 (d, 2H, CH_2, J = 14 Hz), 2.15 (br, 2H, CH_2, J = 14 Hz), 2.54 (d, 2H, CH_2, J = 14 Hz), 4.40 (d, 2H, CH_2, J = 15 Hz), 5.03 (d, 2H, CH_2, J = 15 Hz), 6.65−8.23 (m, 60H, ArH). ^{31}P{^{1}H} NMR (121 MHz, CD_2Cl_2, r.t.): δ −47.6 (m, 2P, P_C),−11.8 to −6.3 (m, 4P), −4.4 (m, 2P). ESI−MS (in CH_2Cl_2): m/z 735.143 (z = 2, [Pd_2(dpmppm)$_2$]$^{2+}$ (735.082)), 1557.311 (z = 1, {[Pd_2(dpmppm)$_2$]BF_4}$^+$ (1557.168)). IR (KBr): ν 1436 (s, P−C), 1139 (w), 1378 (m), 1309 (m), 1281 (w), 1191 (w), 1057 (s), 812 (s), 742 (s), 697 (s), 512 (m), 488 (m) cm^{-1}. UV−vis (CH_2Cl_2, r.t.): λ_{max} (log ε) 458 (4.30), 329 (3.93) nm. Anal. Calcd for $C_{78.5}H_{73}B_2ClF_8P_8Pd_2$ ([**1**]$(BF_4)_2$·0.5CH_2Cl_2): C, 55.92; H, 4.36%. Found: C, 55.76; H, 4.33%.

Preparation of [Pd_4(μ-dpmppm)$_2$(XylNC)$_3$]$(PF_6)_2$ ([3a]$(PF_6)_2$). Portions of [**2**]$(PF_6)_2$·CH_2Cl_2 (149 mg, 85 μmol) and [Pd_3(XylNC)$_6$] (62 mg, 56 μmol) (or [Pd(dba)$_2$] (168 μmol) and XylNC (336 μmol)) were dissolved in 2 mL of acetonitrile, which was heated at 60 °C for 5 h to afford a dark bluish green solution. The reaction mixture was filtered, and careful addition of Et_2O to the solution yielded a green powder of [**3a**]$(PF_6)_2$, which were collected by filtration, washed with Et_2O, and dried under a vacuum. Yield: 69 mg, 33% (vs Pd). ^{1}H NMR (300 MHz, CD_3CN, 60 °C): δ 1.82 (s, 18H, CH_3), 2.81 (dt, 2H, CH_2, J_{HH} = 14, 4 Hz), 3.77 (d, 4H, CH_2, J_{HH} = 14 Hz), 3.92 (m, 2H, CH_2, J_{HH} = 14, 4 Hz), 4.01 (d, 4H, CH_2, J_{HH} = 14 Hz), 6.43−7.29 (m, 69H, ArH). ^{1}H NMR (300 MHz, CD_3CN, 20 °C): δ 1.70 (s, 18H, C_{H3}), 2.29 (s, 2H, CH_2), 3.72 (s, 4H, CH_2), 3.88−3.96 (m, 6H, CH_2), 6.58−7.77 (m, 69H, ArH). ^{1}H NMR (300 MHz, CD_3CN, −30 °C): δ 3.83−3.69 (br, 12H, CH_2), 7.81−6.54 (br, 69H, ArH). ^{31}P{^{1}H} NMR (121 MHz, CD_3CN, 60 °C): δ −144.8 (sep, 2P, $^1J_{PF}$ = 713 Hz), −12.0 (q, 4P), −1.1 (q, 4P); (121 MHz, CD_3CN, 20 °C): δ −144.7 (sep, 2P, $^1J_{PF}$ = 713 Hz), −11.4 (s, 4P), −1.4 (s, 4P). ^{31}P{^{1}H} NMR (121 MHz, CD_3CN, −30 °C): δ −144.82 (sep, 2P, $^1J_{PF}$ = 713 Hz), −18.1 (br, 2P), −7.3 (br, 3P), 0.2 (br, 1P), 4.5 (br, 2P). ESI−MS (in CH_3CN): m/z 972.642 (z = 2, {[Pd_4(dpmppm)$_2$(XylNC)$_2$]$^{2+}$ (972.560)). IR (KBr): 2130, 2098, 2040 (C≡N), 1436 (s, P−C), 1096 (m), 838 (s, PF_6), 779 (m), 741 (m), 693 (m) cm^{-1}. UV−vis (CH_2Cl_2, 60 °C): λ_{max} (log ε) 672 (4.69) nm. UV−vis (CH_2Cl_2, 20 °C): 669 (4.79). UV−vis (CH_2Cl_2, −30 °C): 659 (4.64) nm. Anal. Calcd for $C_{105}H_{98}N_3F_{12}P_{10}Pd_2$ ([**3a**]$(PF_6)_2$): C, 53.29; H, 4.22; N, 1.78%. Found: C, 53.06; H, 3.98; N, 1.85%.

Preparations of [Pd_4(μ-dpmppm)$_2$(^{t}BuNC)$_2$]$(PF_6)_2$ ([3b′]$(PF_6)_2$). An acetonitrile solution (2 mL) containing [**2**]$(PF_6)_2$·CH_2Cl_2 (154 mg, 88 μmol), [Pd(dba)$_2$] (101 mg, 175 μmol), and ^{t}BuNC (22 μL, 195 μmol) was heated at 60 °C for 5 h to afford a dark bluish green solution. The solution was filtered, and careful addition of Et_2O to the solution gave a green powder of [**3b′**]$(PF_6)_2$, which were collected by filtration, washed with Et_2O, and dried under a vacuum. Yield: 35 mg, 19% (vs Pd). Anal. Calcd for $C_{88}H_{93}N_2F_{12}P_{10}Pd_2$ ([**3b′**]$(PF_6)_2$): C, 49.41; H, 4.24; N, 1.31%. Found: C, 49.19; H, 4.01; N, 1.50%. IR (KBr): 2171 (C≡N), 1435 (s, P−C), 1098 (m), 839 (s, PF_6), 741 (m), 692 (m), 557 (m) cm^{-1}. The UV−vis, ^{1}H and ^{31}P{^{1}H} NMR, and ESI−MS spectral data of [**3b′**]$(PF_6)_2$ were measured on acetonitrile solutions in the presence of 1 equiv of ^{t}BuNC. UV−vis (in CH_3CN, 60 °C): λ_{max} (log ε) 675 (4.69) nm. UV−vis (in CH_3CN, 20 °C): 673 (4.79). UV−vis (in CH_3CN, −30 °C): 665 (4.64) nm. ^{1}H NMR (300 MHz, CD_3CN, 60 °C): δ 1.10 (s, 18H CH_3), 2.52 (dt, 2H CH_2, J = 15, 3 Hz), 3.68 (d, 4H CH_2, J = 15 Hz), 3.79 (d, 2H CH_2, J = 15, 3 Hz), 4.03 (d, 4H, CH_2, J = 15, 3 Hz), 6.61−8.13 (m, 60H, ArH). ^{1}H NMR (CD_3CN, 20 °C): δ 1.08 (s, 18H CH_3), 2.29 (br d, 2H CH_2), 3.60 (br d, 4H, CH_2), 3.88−3.96 (m, 6H, CH_2), 6.63−7.76 (m, 60H, ArH). ^{1}H NMR (CD_3CN, −30 °C): δ 1.20 (br, 18H, CH_3), 2.63 (br, 2H, CH_2), 3.35−3.86 (br, 10H, CH_2), 6.42−7.77 (br, 60H, ArH). ^{31}P{^{1}H} NMR (121 MHz, CD_3CN, 60 °C): δ −144.1 (sep, 2P, $^1J_{P-F}$ = 713 Hz), −11.9 (q, 4P), −0.1 (q, 4P). ^{31}P{^{1}H} NMR (121 MHz, CD_3CN, 20 °C): δ −144.1 (sep, 2P, $^1J_{P-F}$ = 713 Hz), −10.9 (s, 4P), −0.7 (s, 4P). ^{31}P{^{1}H} NMR (121 MHz, CD_3CN, −30 °C): δ −144.4 (sep, 2P, $^1J_{P-F}$ = 713 Hz), −15.3 (br, 2P), −6.6 − −1.3 (br, 4P), 4.1 (br, 2P). ESI−MS (in CH_3CN): m/z 924.506 (z = 2, [Pd_4(dpmppm)$_2$(^{t}BuNC)$_2$]$^{2+}$ (924.560)).

Preparations of [Pd_8(μ-dpmppm)$_4$(CH_3CN)$_2$]X_4 ([4]X_4, X = BF_4, PF_6). To a solution of [**2**]$(BF_4)_2$·0.5CH_2Cl_2 (131 mg, 80 μmol) in acetonitrile (7.5 mL) was added [Pd(dba)$_2$] (91 mg, 159 μmol), and the reaction mixture was heated at 60 °C for 3 h. The solution was passed through a membrane filter and concentrated to ca. 5 mL. The addition of Et_2O (20 mL) yielded a green powder of [**4**]$(BF_4)_4$,[11] which was collected by filtration, washed with Et_2O, and dried under a vacuum. Yield: 54% (vs Pd determined by ^{31}P NMR). The powder was recrystallized from an acetonitrile (5 mL) and diethyl ether (3 mL) mixed solvent to afford block-shaped crystals of [**4**]$(BF_4)_4$ in 13% yield. The isolated compound was analyzed by IR, UV−vis−NIR, ^{1}H and ^{31}P{^{1}H} NMR, and ESI−MS spectroscopy.[11]

To a solution of [**2**]$(PF_6)_2$·CH_2Cl_2 (101 mg, 57 μmol) in acetonitrile (7.5 mL) was added [Pd(dba)$_2$] (66 mg, 115 μmol), and the reaction mixture was heated at 60 °C for 3 h. The solution was passed through a membrane filter and concentrated to ca. 5 mL. The addition of Et_2O (20 mL) gave a green powder of [**4**]$(PF_6)_4$, which was collected by filtration, washed with Et_2O, and dried under a vacuum. Yield: 58% (vs Pd determined by ^{31}P NMR). The powder was recrystallized from an acetonitrile (5 mL) and diethyl ether (2 mL) mixed solvent to afford pale brown block-shaped crystals of [**4**]$(PF_6)_4$·Et_2O in 8% isolated yield. Anal. Calcd for $C_{164}H_{160}ON_2F_{24}P_{20}Pd_8$ ([**4**]$(PF_6)_4$·Et_2O): C, 48.21; H, 3.87; N, 0.47%. Found: C, 48.02; H, 3.93; N, 0.68%. IR (KBr): 1483 (m), 1436 (s, P−C), 1099 (m), 840 (s, PF_6), 795 (m), 740 (s), 691 (m), 557 (m), 514 (m), 476 (m) cm^{-1}. UV−vis (in CH_3CN, 60 °C): λ_{max} (log ε) 639 (5.07) nm; (in CH_3CN, 25 °C): 900 (4.98), 633 (4.94). UV−vis (in CH_3CN, −30 °C): 896 (5.43) nm. ^{1}H NMR (300 MHz, CD_3CN, 20 °C): δ 0.85 (d, 4H CH_2, $^2J_{HH}$ = 13 Hz), 1.02 (d, 4H CH_2, $^2J_{HH}$ = 14 Hz), 1.95 (s, 6H CH_3CN), 3.01 (d, 4H CH_2, $^2J_{HH}$ = 14 Hz), 3.20 (d, 4H CH_2, $^2J_{HH}$ = 14 Hz), 3.32 (d, 4H CH_2, $^2J_{HH}$ = 13 Hz), 3.41 (d, 4H CH_2, $^2J_{HH}$ = 14 Hz), 5.98−7.82 (m, 120H, ArH). ^{31}P{^{1}H} NMR (121 MHz, CD_3CN, 20 °C): δ −144.3 (sep, 2P, $^1J_{P-F}$ = 713 Hz), −15.6 (q, 4P), −9.0 (m, 4P), −6.1 (m, 4P), 2.5 (m, 4P). ESI−MS (in CH_3CN): m/z 1827.5117 (z = 1, {[Pd_4(dpmppm)$_2$]PF_6}$^+$ (1826.937)), 841.068 (z = 2, [Pd_4

DOI: 10.1021/acs.inorgchem.5b00950
Inorg. Chem. 2015, 54, 8298−8309

$(dpmppm)_2]^{2+}$ (840.986)). Note that $[4](PF_6)_4$ was able to be prepared by the previously reported procedure,[11] heating a 1:2 mixture of dpmppm and $[Pd(dba)_2]$ in acetonitrile at 60 °C for 3 h in the presence of 1 equiv of $[Cu(CH_3CN)_4]PF_6$.

Preparations of $[Pd_2Cl(Cp^*M'Cl_2)(Cp^*M'Cl)(\mu\text{-dpmppm})_2](PF_6)_2$ (M′ = Rh ($[5](PF_6)_2$), Ir ($[6](PF_6)_2$)). To a solution of $[2](PF_6)_2\cdot CH_2Cl_2$ (46 mg, 26 μmol) in CH_2Cl_2 (10 mL) was added $[Cp^*RhCl_2]_2$ (17 mg, 27 μmol), and the reaction mixture was stirred for 12 h at room temperature. The solvent was removed to dryness, and the residue was extracted with CH_2Cl_2 (5 mL), which was filtered and concentrated to ca. 3 mL. After the addition of Et_2O (2 mL), the solution was allowed to stand in a refrigerator to yield red crystals of $[5](PF_6)_2\cdot CH_2Cl_2$, which were collected by filtration, washed with Et_2O, and dried under a vacuum. Yield: 29 mg, 47% (vs Pd). ^{1}H NMR (300 MHz, CD_2Cl_2, r.t.): δ 1.42 (d, $^4J_{PH}$ = 4 Hz, 15H, Cp*), 1.49 (t, $^4J_{PH}$ = 4 Hz, 15H, Cp*), 2.1−4.9 (m, br, 12H, CH_2), 6.4−7.8 (m, 60H, Ar*H*). ^{31}P{^{1}H} NMR (121 MHz, CD_2Cl_2, r.t.): δ −144.2 (sep, $^1J_{PF}$ = 711 Hz, 2P, PF_6), −19.0 (m, 1P, P_{D2}), −18.7 (m, $^1J_{PP}'$ = 425 Hz, 2P, P_{B2}), −10.7 (m, $^1J_{RhP}$ = 109 Hz, $^2J_{PP}'$ = 103 Hz, 1P, P_{C1}), −8.19 to −3.74 (m, $^2J_{PP}'$ = 381 Hz, 2P, P_{A2}, P_{B1}), −2.68 (m, $^2J_{PP}'$ = 408 Hz, 1P, P_{A1}), 1.89 (dd, $^2J_{PP}'$ = 23, 16 Hz, 1P, P_{D1}), 20.1 (ddd, $^1J_{RhP}$ = 114 Hz, $^2J_{PP}'$ = 103 Hz, 1P, P_{C2}). ESI−MS (in CH_2Cl_2/CH_3OH): *m*/*z* 2231.665 (*z* = 1, $\{[Pd_2Cl(Cp^*RhCl_2)(Cp^*RhCl)(dpmppm)_2]PF_6\}^+$ (2232.040)). IR (KBr): 1436 (s, P−C), 1098 (m), 842 (s, PF_6), 739 (m), 692 (m), 557 (m) cm^{-1}. UV−vis (in CH_2Cl_2 at r.t.): λ_{max}/nm (log ε) 465 (4.27), 390 (4.41), 347 (4.39) nm. Anal. Calcd for $C_{99}H_{104}Cl_6F_{12}P_{10}Pd_2Rh_2$ ($[5](PF_6)_2\cdot CH_2Cl_2$): C, 48.28; H, 4.26%. Found: C, 48.20; H, 3.91%.

Complex $[6](PF_6)_2$ was prepared by a procedure similar to that of $[5](PF_6)_2$, using $[2](PF_6)_2\cdot CH_2Cl_2$ (33 mg, 19 μmol) and $[Cp^*IrCl_2]_2$ (15 mg, 19 μmol). Orange crystals of $[6](PF_6)_2\cdot CH_2Cl_2$ were obtained in 52% yield (25 mg). ^{1}H NMR (300 MHz, CD_2Cl_2, r.t.): δ 1.30 (d, $^4J_{PH}$ = 3 Hz, 15H, Cp*), 1.50 (t, $^4J_{PH}$ = 3 Hz, 15H, Cp*), 2.1−5.4 (m, br, 12H, CH_2), 6.4−8.4 (m, 60H, Ar*H*). ^{31}P{^{1}H} NMR (121 MHz, CD_2Cl_2, r.t.): δ −144.2 (sep, $^1J_{PF}$ = 711 Hz, 2P, PF_6), −48.6 (ddd, $^2J_{PP}'$ = 61, 45, 7 Hz, 1P, P_{C1}), −29.4 (d, $^2J_{PP}'$ = 61 Hz, 1P, P_{D1}), −21.5 to −17.2 (m, 2P, P_{B2}, P_{D2}), −11.2 (dd, $^2J_{PP}'$ = 16, 10 Hz, 1P, P_{C2}), −9.68 to −3.48 (m, 2P, P_{A2}, P_{B1}), −2.95 (m, $^1J_{PP}'$ = 408 Hz, 1P, P_{A1}). ESI−MS (in CH_2Cl_2/CH_3OH): *m*/*z* 2411.942 (*z* = 1, $\{[Pd_2Cl(Cp^*IrCl_2)(Cp^*IrCl)(dpmppm)_2]PF_6\}^+$ (2411.161)). IR (KBr): 1436 (s, P−C), 1096 (m), 840 (s, PF_6), 742 (m), 694 (m), 557 (m) cm^{-1}. UV−vis (in CH_2Cl_2 at r.t.): λ_{max}/nm (log ε) 464 (3.02), 391 (4.05), 342 (4.19) nm. Anal. Calcd for $C_{99}H_{104}Cl_6F_{12}P_{10}Pd_2Ir_2$ ($[6](PF_6)_2\cdot CH_2Cl_2$): C, 45.01; H, 3.97%. Found: C, 45.14; H, 3.79%.

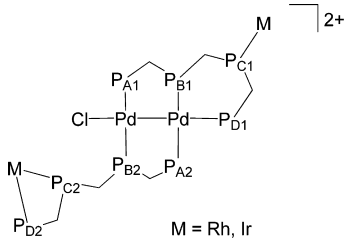

Preparation of $[Au_2Pd_2Cl_2(dpmppm-H)_2](PF_6)_2$ ($[7](PF_6)_2$). To a solution of $[2](PF_6)_2\cdot CH_2Cl_2$ (100 mg, 57 μmol) in CH_2Cl_2 (20 mL) was added $[AuCl(PPh_3)]$ (56 mg, 113 μmol), and the reaction mixture was stirred overnight at room temperature. The solvent was removed to dryness, and the residue was washed with Et_2O (20 mL) and extracted with CH_2Cl_2 (20 mL), which was filtered and concentrated to ca. 8 mL. After the addition of Et_2O (5 mL), the solution was allowed to stand in a refrigerator to yield yellow crystals of $[7](PF_6)_2\cdot 2CH_2Cl_2$, which were collected by filtration, washed with Et_2O, and dried under a vacuum. Yield: 8.6 mg, 7% (vs Pd). ^{1}H NMR (300 MHz, CD_2Cl_2, r.t.): δ 3.40 (d, $^2J_{HH}$ = 15 Hz, 4H, CH_2), 3.97 (d, $^2J_{HH}$ = 15 Hz, 4H, CH_2), 4.85 (s, 2H, C*H*), 7.08−8.07 (m, 60H, Ar*H*). ^{31}P{^{1}H} NMR (121 MHz, CD_2Cl_2, r.t.): δ −144.2 (sep, $^1J_{PF}$ = 711 Hz, 2P, PF_6), 11.1 (m, 4P), 44.6 (m, 4P). ESI−MS (in CH_2Cl_2): *m*/*z* 966.038 (*z* = 2, $[Au_2Pd_2Cl_2(dpmppm-H)_2]^{2+}$ (966.009)), 2077.061 (*z* = 1, $\{[Au_2Pd_2Cl_2(dpmppm-H)_2]PF_6\}^+$ (2076.982)). IR (KBr): 1484 (m), 1436 (s, P−C), 1372 (w), 1101 (s), 839 (s, PF_6), 804 (m), 733 (m), 688 (s), 557 (m), 480 (m) cm^{-1}. UV−vis (CH_2Cl_2, r.t.): λ_{max}/nm (log ε) 474 (4.37), 390 (4.41), 347 (4.39) nm. Since $[7](PF_6)_2\cdot 2CH_2Cl_2$ was obtained with a small amount of inorganic impurity, the formula was determined by an X-ray crystallographic analysis.

X-ray Crystallographic Analyses of $[1](PF_6)_2$, $[2](PF_6)_2\cdot CH_2Cl_2$, $[5](PF_6)_2\cdot 7CH_2Cl_2\cdot Et_2O$, $[6](PF_6)_2\cdot 3.5CH_2Cl_2$, and $[7](PF_6)_2\cdot 2CH_2Cl_2$. The crystals of $[1](PF_6)_2$, $[2](PF_6)_2\cdot CH_2Cl_2$, $[5](PF_6)_2\cdot 7CH_2Cl_2\cdot Et_2O$, $[6](PF_6)_2\cdot 3.5CH_2Cl_2$, and $[7](PF_6)_2\cdot 2CH_2Cl_2$ were quickly coated with Paratone N oil and mounted on top of a loop fiber at room temperature. Reflection data were collected at low temperature with a Rigaku VariMax Mo/Saturn CCD diffractometer equipped with graphite-monochromated confocal Mo Kα radiation using a rotating-anode X-ray generator RA-Micro7 (50 kV, 24 mA). Crystal and experimental data are summarized in Tables S1 and S2. All data were collected at −120 °C ($[1](PF_6)_2$, $[2](PF_6)_2$, $[5](PF_6)_2$, and $[6](PF_6)_2$) and −150 °C ($[7](PF_6)_2$), and a total of 2160 oscillation images, covering a whole sphere of 6° < 2θ < 55°, were corrected by the ω-scan method (−62° < ω < 118°) with a Δω of 0.25°. The crystal-to-detector (70 × 70 mm) distance was set at 60 mm. The data were processed using the *Crystal Clear 1.3.5* program (Rigaku/MSC)[26] and corrected for Lorentz polarization and absorption effects.[27] The structures of complexes were solved by direct methods with *SHELXS-97*[28a] and *SIR-92*,-97[29] and were refined on F^2 with full-matrix least-squares techniques with *SHELXL-97*[28b] using the *Crystal Structure 3.7* package.[30] All non-hydrogen atoms were refined with anisotropic thermal parameters, and the C−H hydrogen atoms except those for some disordered phenyl and solvent molecules ($[5](PF_6)_2$ and $[7](PF_6)_2$) were calculated at ideal positions and refined with riding models. In the structures of $[5](PF_6)_2$, one dichloromethane molecule of crystallization is disordered, and in $[7](PF_6)_2$, the Pd-coordinated chloride atom (Cl1, Cl2) and three phenyl groups on P2, P3, and P4 atoms are refined as disordered at two sites with half occupancy, and the dichloromethane molecule is also disordered. The crystals of $[7](PF_6)_2$ were notably very unstable at room temperature owing to the disordered structure, which led to somewhat low-grade crystallographic results. All calculations were carried out on a Windows PC with the *Crystal Structure 3.7* package.[30]

■ ASSOCIATED CONTENT

Supporting Information

The Supporting Information is available free of charge on the ACS Publications website at DOI: 10.1021/acs.inorgchem.5b00950.

Tables of crystallographic data of $[1](PF_6)_2$, $[2](PF_6)_2$, $[5](PF_6)_2$, $[6](PF_6)_2$, and $[7](PF_6)_2$; curve-fitting results for titration; ORTEP diagrams of $[1](PF_6)_2$, $[6](PF_6)_2$, and $[7](PF_6)_2$; CV of $[2](PF_6)_2$; ^{31}P{^{1}H} NMR spectra of $[1](PF_6)_2$, $[2]X_2$, $[3b']PF_6)_2$, $[3a](PF_6)_2$, $[5](PF_6)_2$, $[6](PF_6)_2$, and $[7](PF_6)_2$; VT ^{31}P{^{1}H} NMR spectra of $[3Fa](PF_6)_2$ and $[3Fb](PF_6)_2$; VT ^{1}H{^{31}P} NMR spectra of $[3a](PF_6)_2$ and $[3b'](PF_6)_2$ with ^{t}BuNC; ^{1}H{^{31}P} NMR spectrum of $[7](PF_6)_2$; ESI-MS of $[1](PF_6)_2$, $[2]X_2$, $[3b']PF_6)_2$, $[3a](PF_6)_2$, $[4](PF_6)_2$, $[5](PF_6)_2$, $[6](PF_6)_2$, and $[7](PF_6)_2$; and electronic absorption spectral changes for reactions of $[3b']PF_6)_2$, $[3Fb](PF_6)_2$ with ^{t}BuNC, and $[4](PF_6)_2$ (PDF)

CIF file giving the structural parameters of $[1](PF_6)_2$, $[2](PF_6)_2$, and $[5](PF_6)_2$ (CIF)

CIF file giving the structural parameters of $[6](PF_6)_2$ and $[7](PF_6)_2$ (CIF)

DOI: 10.1021/acs.inorgchem.5b00950
Inorg. Chem. 2015, 54, 8298−8309

AUTHOR INFORMATION

Corresponding Author

*Tel.: +81 742-20-3399. Fax +81 742-20-3847. E-mail: tanase@cc.nara-wu.ac.jp.

Notes

The authors declare no competing financial interest.

ACKNOWLEDGMENTS

This work was supported by Grant-in-Aid for Scientific Research (no. 26288025) and that on Priority Area 2107 (no. 22108521, 24108727) from the Ministry of Education, Culture, Sports, Science and Technology, Japan. T.T. is grateful to Nara Women's University for a research project grant. K.N. is grateful for a JSPS fellowship.

REFERENCES

(1) (a) Yeh, C.-Y.; Wang, C.-C.; Chen, C.-H.; Peng, S.-M. In *Redox Systems under Nano-Space Control*; Hirao, T., Ed.; Springer: Berlin, 2006; pp 85−117 and references cited therein. (b) Berry, J. F. In *Multiple Bond between Metal Atoms*, 3rd ed; Cotton, F. A., Murillo, C. A., Walton, R. A., Eds.; Springer: New York, 2005; pp 669−706, and references cited therein. (c) Liu, I. P.-C.; Wang, W.-Z.; Peng, S.-M. *Chem. Commun.* **2009**, 4323. (d) Chen, C.-H.; Hung, R. D.; Wang, W.-Z.; Peng, S.-M.; Chen, I.-C. *ChemPhysChem* **2010**, *11*, 466. (e) Ismailov, R.; Wang, W.-Z.; Wang, R.-R.; Huang, Y.- L.; Yeh, C.-Y.; Lee, G.-H.; Peng, S.-M. *Eur. J. Inorg. Chem.* **2008**, *2008*, 4290. (f) Peng, S.-M.; Wang, C.-C.; Jang, Y.-L.; Chen, Y.-H.; Li, F.-Y.; Mou, C.-Y.; Leung, M.-K. *J. Magn. Magn. Mater.* **2000**, *209*, 80.

(2) (a) Zhang, T.; Drouin, M.; Harvey, P. D. *Inorg. Chem.* **1999**, *38*, 957. (b) Zhang, T.; Drouin, M.; Harvey, P. D. *Inorg. Chem.* **1999**, *38*, 1305.

(3) Murahashi, T.; Mochizuki, E.; Kai, Y.; Kurosawa, H. *J. Am. Chem. Soc.* **1999**, *121*, 10660.

(4) (a) Murahashi, T.; Shirato, K.; Fukushima, A.; Takase, K.; Suenobu, T.; Fukuzumi, S.; Ogoshi, S.; Kurosawa, H. *Nat. Chem.* **2012**, *4*, 52. (b) Murahashi, T.; Inoue, R.; Usui, K.; Ogoshi, S. *J. Am. Chem. Soc.* **2009**, *131*, 9888. (c) Tatsumi, Y.; Naga, T.; Nakashima, H.; Murahashi, T.; Kurosawa, H. *Chem. Commun.* **2008**, 477. (d) Murahashi, T.; Kato, N.; Uemura, T.; Kurosawa, H. *Angew. Chem., Int. Ed.* **2007**, *46*, 3509. (e) Murahashi, T.; Fujimoto, M.; Oka, M.; Hashimoto, Y.; Uemura, T.; Tatsumi, Y.; Nakao, Y.; Ikeda, A.; Sakai, S.; Kurosawa, H. *Science* **2006**, *313*, 1104. (f) Tatsumi, Y.; Shirato, K.; Murahashi, T.; Ogoshi, S.; Kurosawa, H. *Angew. Chem., Int. Ed.* **2006**, *45*, 5799. (g) Tatsumi, Y.; Murahashi, T.; Okada, M.; Ogoshi, S.; Kurosawa, H. *Chem. Commun.* **2004**, 1430. (h) Murahashi, T.; Uemura, T.; Kurosawa, H. *J. Am. Chem. Soc.* **2003**, *125*, 8436. (i) Murahashi, T.; Higuchi, Y.; Katoh, T.; Kurosawa, H. *J. Am. Chem. Soc.* **2002**, *124*, 14288. (j) Murahashi, T.; Nagai, T.; Okuno, T.; Matsutani, T.; Kurosawa, H. *Chem. Commun.* **2000**, 1689.

(5) Ismayilov, R. H.; Wang, W.-Z.; Lee, G.-H.; Yeh, C.-Y.; Hua, S.-A.; Song, Y.; Rohmer, M.-M.; Bénard, M.; Peng, S.-M. *Angew. Chem., Int. Ed.* **2011**, *50*, 2045.

(6) Horiuchi, S.; Tachibana, Y.; Yamashita, M.; Yamamoto, K.; Masai, K.; Takase, K.; Matsutani, T.; Kawamata, S.; Kurashige, Y.; Yanai, T.; Murahashi, T. *Nat. Commun.* **2015**, *6*, 6742.

(7) (a) Tanase, T.; Ukaji, H.; Takahata, H.; Toda, H.; Igoshi, T.; Yamamoto, Y. *Organometallics* **1998**, *17*, 196. (b) Tanase, T. *Bull. Chem. Soc. Jpn.* **2002**, *75*, 1407. (c) Tanase, T.; Hamaguchi, M.; Begum, R. A.; Yano, S.; Yamamoto, Y. *Chem. Commun.* **1999**, 745. (d) Tanase, T.; Ukaji, H.; Igoshi, T.; Yamamoto, Y. *Inorg. Chem.* **1996**, *35*, 4114. (e) Tanase, T.; Hamaguchi, M.; Begum, R. A.; Goto, E. *Chem. Commun.* **2001**, 1072. (f) Tanase, T.; Goto, E.; Begum, R. A.; Hamaguchi, M.; Zhan, S.; Iida, M.; Sakai, K. *Organometallics* **2004**, *23*, 5975. (g) Hosokawa, A.; Kure, B.; Nakajima, T.; Nakamae, K.; Tanase, T. *Organometallics* **2011**, *30*, 6063.

(8) (a) Goto, E.; Begum, R. A.; Zhan, S.; Tanase, T.; Tanigaki, K.; Sakai, K. *Angew. Chem., Int. Ed.* **2004**, *43*, 5029. (b) Goto, E.; Begum, R.; Hosokawa, A.; Yamamoto, C.; Kure, B.; Nakajima, T.; Tanase, T. *Organometallics* **2012**, *31*, 8482. (c) Goto, E.; Begum, R.; Ueno, C.; Hosokawa, A.; Yamamoto, C.; Nakamae, K.; Kure, B.; Nakajima, T.; Kajiwara, T.; Tanase, T. *Organometallics* **2014**, *33*, 1893.

(9) (a) Takemura, Y.; Takenaka, H.; Nakajima, T.; Tanase, T. *Angew. Chem., Int. Ed.* **2009**, *48*, 2157. (b) Takemura, Y.; Nakajima, T.; Tanase, T. *Eur. J. Inorg. Chem.* **2009**, *2009*, 4820. (c) Takemura, Y.; Nakajima, T.; Tanase, T. *Dalton Trans.* **2009**, 10231. (d) Tanase, T.; Otaki, R.; Nishida, T.; Takenaka, H.; Takemura, Y.; Kure, B.; Nakajima, T.; Kitagawa, Y.; Tsubomura, T. *Chem. - Eur. J.* **2014**, *20*, 1577. (e) Takemura, Y.; Nishida, T.; Kure, B.; Nakajima, T.; Iida, M.; Tanase, T. *Chem. - Eur. J.* **2011**, *17*, 10528. (f) Yoshii, A.; Takenaka, H.; Nagata, H.; Noda, S.; Nakamae, K.; Kure, B.; Nakajima, T.; Tanase, T. *Organometallics* **2012**, *31*, 133.

(10) (a) Nakajima, T.; Sakamoto, M.; Kurai, S.; Kure, B.; Tanase, T. *Chem. Commun.* **2013**, *49*, 5239. (b) Nakajima, T.; Kurai, S.; Noda, S.; Zouda, M.; Kure, B.; Tanase, T. *Organometallics* **2012**, *31*, 4283.

(11) Nakamae, K.; Takemura, Y.; Kure, B.; Nakajima, T.; Kitagawa, Y.; Tanase, T. *Angew. Chem., Int. Ed.* **2015**, *54*, 1016.

(12) Tanase, T.; Hatada, S.; Mochizuki, A.; Nakamae, K.; Kure, B.; Nakajima, T. *Dalton Trans.* **2013**, *42*, 15941.

(13) (a) Tanase, T.; Kawahara, K.; Ukaji, H.; Kobayashi, K.; Yamazaki, H.; Yamamoto, Y. *Inorg. Chem.* **1993**, *32*, 3682. (b) Tanase, T.; Ukaji, H.; Yamamoto, Y. *J. Chem. Soc., Dalton Trans.* **1996**, 3059. (c) Zhang, J.; Pattacini, R.; Braunstein, P. *Inorg. Chem.* **2009**, *48*, 11954.

(14) DuBois, D. L.; Miedaner, A.; Haltiwanger, R. C. *J. Am. Chem. Soc.* **1991**, *113*, 8753.

(15) Lin, W.; Wilson, S. R.; Girolami, G. S. *Inorg. Chem.* **1994**, *33*, 2265.

(16) Browning, C. S.; Farrar, D. H.; Frankel, D. C.; Vittal, J. J. *Inorg. Chim. Acta* **1997**, *254*, 329.

(17) (a) *Gold Chemistry*, Mohr, F., Ed.; WILEY-VCH, Weinheim, Germany, 2008. (b) *Modern Supramolecular Gold Chemistry*, Laguna, A., Ed.; WILEY-VCH, Weinheim, Germany, 2008. (c) Pyykkö, P. *Chem. Rev.* **1997**, *97*, 597. (b) Pyykkö, P. *Angew. Chem.* **2004**, *116*, 4512.

(18) *Organometallic Pincer Chemistry*, van Koten, G.; Milstein, D., Eds.; Springer-Verlag, Berlin, 2013.

(19) Reitsamer, C.; Stallinger, S.; Schuh, W.; Kopacka, H.; Wurst, K.; Obendorf, D.; Peringer, P. *Dalton. Trans.* **2012**, *41*, 3503.

(20) Neo, K. E.; Huynh, H. V.; Koh, L. L.; Henderson, W.; Hor, T. S. A. *J. Organomet. Chem.* **2008**, *693*, 1628.

(21) Cherwinski, W. J.; Johnson, B. F. G.; Lewis, J. *J. Chem. Soc., Dalton Trans.* **1974**, 1405.

(22) Christofides, A. *J. Organomet. Chem.* **1983**, *259*, 355.

(23) Kang, J. W.; Moseley, K.; Maitlis, P. M. *J. Am. Chem. Soc.* **1969**, *91*, 5970.

(24) McAuliffe, C. A.; Parish, R. V.; Randall, P. D. *J. Chem. Soc., Dalton Trans.* **1979**, 1730.

(25) (a) Yamamoto, Y.; Yamazaki, H. *Organometallics* **1993**, *12*, 1833. (b) Yamamoto, Y.; Takahashi, K.; Matsuda, K.; Yamazaki, H. *J. Chem. Soc., Dalton Trans.* **1987**, 1833. (c) Yamamoto, Y.; Takahashi, K.; Yamazaki, H. *J. Am. Chem. Soc.* **1986**, *108*, 1833. (d) Yamamoto, Y.; Takahashi, K.; Yamazaki, H. *Chem. Lett.* **1985**, 201. (e) Boehm, J. R.; Balch, A. L. *Inorg. Chem.* **1977**, *14*, 778. (f) Rettig, M. F.; Kirk, E. A.; Maitlis, P. M. *J. Organomet. Chem.* **1976**, *111*, 113.

(26) *Crystal Clear*, version 1.3.5; Operating software for the CCD detector system; Rigaku and Molecular Structure Corp., Tokyo, Japan; The Woodlands, TX, 2003.

(27) Jacobson, R. *REQAB*; Molecular Structure Corporation, The Woodlands, Texas, 1998.

(28) (a) Sheldrick, G. M. *SHELXS-97*; Program for the Solution of Crystal Structures; University of Göttingen: Göttingen, Germany, 1996. (b) Sheldrick, G. M. *SHELXL-97*; Program for the Refinement of Crystal Structures; University of Göttingen: Göttingen, Germany, 1996.

(29) (a) Altomare, A.; Burla, M. C.; Camalli, M.; Cascarano, M.; Giacovazzo, C.; Guagliardi, A.; Polidori, G. *J. Appl. Crystallogr.* **1994**,

DOI: 10.1021/acs.inorgchem.5b00950
Inorg. Chem. 2015, 54, 8298−8309

27, 435. (b) Altomare, A.; Burla, M.; Camalli, M.; Cascarano, G.; Giacovazzo, C.; Guagliardi, A.; Moliterni, A.; Polidori, G.; Spagna, R. *J. Appl. Crystallogr.* **1999**, *32*, 115.
(30) *Crystal Structure 3.7 and 4.0: Crystal Structure Analysis Package*; Rigaku Corporation: Tokyo, Japan, 2000.

DOI: 10.1021/acs.inorgchem.5b00950
Inorg. Chem. 2015, 54, 8298−8309